2017년 2월
석사학위 논문

Studies on Asymmetric Distribution of RapGAP3 during Cell Migration in *Dictyostelium* and Fucoidan-Mediated Cell Polarization in Osteoblasts

조선대학교 대학원

생명과학과

김 혜 선

Studies on Asymmetric Distribution of RapGAP3 during Cell Migration in *Dictyostelium* and Fucoidan-Mediated Cell Polarization in Osteoblasts

Dictyostelium에서 세포이동 시 **RapGAP3** 단백질의 비대칭적 배열과 **Osteoblast**에서 후코이단 매개 세포 극성화 연구

2017 년 2 월 24 일

조선대학교 대학원

생명과학과

김 혜 선

Studies on Asymmetric Distribution of RapGAP3 during Cell Migration in *Dictyostelium* and Fucoidan-Mediated Cell Polarization in Osteoblasts

지도교수 전 택 중

이 논문을 이학석사학위 신청 논문으로 제출함

2016 년 10월

조선대학교 대학원

생명과학과

김 혜 선

김혜선의 석사학위논문을 인준함

위원장 조선대학교 부교수 이 준 식 (인)

위 원 조선대학교 부교수 이 성 행 (인)

위 원 조선대학교 부교수 전 택 중 (인)

2016년 11월

조선대학교 대학교

CONTENTS

LIST OF FIGURES

PART I. Study on Asymmetric Distribution of RapGAP3 During Cell Migration in *Dictyostelium*

PART II. Study on Fucoidan-Mediated Cell Polarization in Osteoblasts

LIST OF TABLES

ABBREVIATIONS

ABD	Actin binding domain
ABP	Actin binding protein
ADP	Adenosine diphosphate
CON	Control cell
cAMP	Cyclic adenosine monophosphate
FUC	Fucoidan treated cell
GAP	GTPase activating proteins
GDP	Guanosine diphosphate
GFP	Green fluorescent protein
GEF	Guanine nucleotide exchange factor
GTP	Guanosine triphosphate
MAPK	Mitogen activated protein kinase
MTT	3-(4,5-Dimethylthiazol-2-yl)-2,5-diphenyltetrazolium bromide
PBS	Phosphate-buffered saline
PCR	Polymerase chain reaction
PH	Pleckstrin homology
PI	Propidium iodied
PI3K	Phosphatidylinositol 3-kinase
SD	Standard deviation
SEM	Standard error of measurement
TRITC	Tetramethylrhodamine

ABSTRACT

Studies on Asymmetric Distribution of RapGAP3 during Cell Migration in *Dictyostelium* and Fucoidan-Mediated Cell Polarization in Osteoblasts

Hyeseon Kim

Advisor : Associate Prof. Taeck Joong Jeon, Ph.D.

Department of Life Science

Graduate School of Chosun University

Establishment of cell polarity is mediated by a series of signaling molecules that are asymmetrically activated or localized in the cell upon extracellular stimulation. However, the molecular mechanism for differential localization of the signaling molecules in the cell in response to chemoattractant stimulation remains largely unknown. Recently, it has been demonstrated that the I/LWEQ domain in RapGAP3 is sufficient for its posterior localization in migrating cells. To understand the mechanism that mediates anterior/posterior asymmetric localization of RapGAP3 during migration, I determined the minimally required amino acids in the I/LWEQ domain that cause posterior localization and found that the minimal region of the F-actin binding domain for posterior localization could, with some additional deletion at the C-terminal, localize to the anterior. Analysis of the localization and translocation kinetics to the cell cortex of the truncated proteins suggests that the required regions for anterior/posterior localization might have a preferential binding affinity to pre-existing F-actins at the rear

and lateral sides of the cell or newly formed F-actins at the front of the cell, leading to distinct differential sites of the cell. These results provide insights into asymmetric localization of the signaling molecules contributing to cell polarity formation.

Fucoidan, a sulfated polysaccharide found in brown algae, possesses various biological activities including anti-inflammatory and anti-cancer effects. Also, it has been reported to induce the differentiation and mineralization of osteoblastic cells. Here I investigated the effects of fucoidan on the morphology and migration of osteoblasts MC3T3-E1 cells. Next, I investigated the effects of fucoidan on the cell growth and morphology of human osteosarcoma MG-63 cells.

In osteoblasts MC3T3-E1 cells, I found that the effects of fucoidan on the migration of osteoblasts vary depending on the conditions under which the cells are treated. A migration assay using cells treated with fucoidan before stable attachment on plates showed slightly increased migration of fucoidan-treated cells compared to control cells, whereas wound healing experiments using stably attached cells exhibited a slightly decreased migration. The fucoidan-treated cells became shrunk and rounded and showed significantly decreased spreading and adhesion compared to control cells. F-actin was highly accumulated at the rounded cell cortex by fucoidan treatment. In study of osteosarcoma MG-63 cells, I found that fucoidan induces cell aggregation and apoptosis in osteosarcoma cells when the cells are treated with fucoidan upon seeding before becoming stably attached to the plates. Typical characteristics of apoptotic cells such as chromatin condensation and nuclear fragmentation were observed in fucoidan-treated cells. The number of annexin V-positive cells was increased by fucoidan treatment in a dose-dependent manner. Consistent with these results, cell viability and growth rate were decreased and cell spreading was inhibited in the presence of fucoidan, leading to rounded morphological changes of the cells. These results demonstrate that fucoidan treatment results in cell aggregation through F-actin accumulation at the rounded cell cortex and apoptosis in osteosarcoma MG-63 cells.

국문초록

*Dictyostelium*에서 세포이동 시 RapGAP3 단백질의 비대칭적 배열과 Osteoblast에서 후코이단 매개 세포 극성화 연구

김 혜 선

지도교수 : 전 택 중

생명과학과

조선대학교 대학원

세포 극성화의 설립은 비대칭적으로 활성화되거나 세포 외 자극에 따라 위치되는 일련의 신호 분자들에 의해 매개된다. 그러나, chemoattractant 자극에 대한 반응으로 세포 내 신호 분자들의 차별적인 localization에 대한 분자적 기전은 크게 알려지지 않다. 최근, RapGAP3의 I/LWEQ 도메인이 이동하는 세포의 posterior localization에 충분하다는 것이 증명되었다. 이동 시 RapGAP3의 anterior/posterior의 비대칭적 localization을 매개하는 기전을 이해하기 위해서, 본 연구에서는 posterior localization의 원인이 되는 I/LWEQ 도메인의 최소한으로 필요한 아미노산을 정했고 posterior localization에 대해 C-말단에서 일부 추가적인 제거로 anterior localization 할 수 있는 F-actin binding domain의 최소한의 범위를 발견했다. truncated protein들의 cell cortex로 localization 및 translocation kinetics의 분석은 세포의 별개의 다른 지역들로

선도되는 anterior/posterior localization에 필요한 영역들이 세포의 뒷면과 측면에 기존의 F-actin 혹은 세포 앞면에서 새로 형성된 F-actin에 선택적인 결합 능력을 가질 수 있다는 것을 의미한다. 본 연구는 세포 극성화 형성에 기여하는 신호 분자들의 asymmetric localization에 대한 통찰력을 제공하고자 한다.

갈조류에서 발견되는 황산다당류인 fucoidan은 항 염증과 항암 효과 등을 포함한 다양한 생물학적 활성을 가지고 있다. 또한 fucoidan은 osteoblastic cells의 differentiation과 mineralization을 유도하는 것으로 알려졌다. 본 연구에서는 osteoblasts MC3T3-E1의 형태와 이동에 대한 fucoidan의 효과를 조사하였다. 다음으로, human osteosarcoma MG-63 cells의 세포 증식과 형태에 대해 fucoidan이 미치는 영향을 조사하였다.

첫 번째 연구에서, fucoidan이 세포에 처리되는 조건에 따라 osteoblasts의 이동에 대한 fucoidan의 효과를 발견하였다. 안정적으로 부착한 세포를 이용한 wound healing assay에서는 감소된 이동을 보인 반면, 플레이트에 세포가 부착하기 전에 fucoidan이 처리된 세포의 migration assay은 대조군에 비해 fucoidan-treated cells의 이동이 증가한 것으로 나타났다. fucoidan-treated cells는 대조군에 비해 둥글고 수축하였으며 adhesion 및 spreading이 크게 감소하였다. F-actin은 fucoidan treatment에 의해 둥글어진 세포의 cortex에 축적되었다. 두 번째 연구에서, fucoidan은 osteosarcoma cells가 plates에 안정적으로 부착하기 전에 처리 될 때 cell aggregation과 apoptosis가 유도한다는 것을 발견하였다. chromatin condensation이나 nuclear fragmentation과 같은 apoptotic cells의 전형적인 특징들이 fucoidan-treated cells에서 관찰되었다. Annexin V-positive cells의 수는 fucoidan 농도 의존적으로 증가하였다. 이러한

결과에 일관되게, cell viability와 growth rate는 감소되었고 fucoidan의 존재는 cell spreading을 억제했으며, rounded morphological changes까지 초래하였다. 이러한 결과들은 osteosarcoma MG-63 세포에서 후코이단 처리는 둥글어진 세포 cortex로의 F-actin 축적과 apoptosis를 초래한다는 것을 설명한다.

PART I. Study on Asymmetric Distribution of RapGAP3 During Cell Migration in *Dictyostelium*

I. Introduction

Directional cell migration is an essential biological process in development, wound healing, immune response, and cancer metastasis (Artemenko et al., 2014; Ridley et al., 2003). For directional migration, cells should first be polarized to form the front and the rear by differentially localizing signaling molecules to the poles of cells. At the front, F-actin is newly polymerized upon stimulation and leads to protrusions, whereas myosin II is assembled at the rear and along the lateral sides of cells and mediates contractions of the cells in a coordinated manner with pre-existing F-actins at the cortex. The asymmetrical localization of cytoskeletal components is driven by a series of signaling molecules that are differentially activated or localized upon extracellular stimulations such as chemoattractants and electrical stimuli (Artemenko et al., 2014; Lee and Jeon, 2012; Ridley et al., 2003). In *Dictyostelium*, an extracellular shallow gradient of the chemoattractant cAMP is detected by G protein-coupled cAMP receptors and is converted into an interior cellular signal, resulting in a steep gradient of cellular components. This internal gradient of signaling molecules, including Ras GTPases, Rac GTPases, phosphatidylinositol 3-kinases (PI3Ks), and TORC2 complexes, induces coordinated remodeling of the cytoskeleton and ultimately directional cell migration (Artemenko et al., 2014; Lee and Jeon, 2012). One of the early intracellular responses displaying distinct asymmetric distribution induced by the shallow gradient of the extracellular chemoattractant cAMP is the activation of Ras proteins. While the cAMP

receptors and G-proteins are almost evenly distributed on the plasma membrane and G-protein activation reflects only the shallow gradient of extracellular cAMP. Ras Proteins such as RasG and Rap1 are rapidly and transiently activated in response to chemoattractant stimulation and are differentially activated at the leading edge of the cell, resulting in establishment of cell polarity and directional cell migration (Artemenko et al., 2014; Jeon et al., 2007b; Kortholt and van Haastert, 2008; Lee and Jeon, 2012; Sasaki et al., 2004). However, the mechanism that leads to the asymmetric activation of the Ras proteins at the leading edge of the cell remains largely unknown.

Rap1 is a key signaling molecule in integrin-mediated cell-substratum adhesion and cadherin-mediated cell-cell adhesion (Kooistra et al., 2007; Retta et al., 2006). The activity of Rap1 is regulated by guanine nucleotide exchange factors (GEFs) and GTPase activating proteins (GAPs) (Fig. 1) (Bos, 2005; Bos and Zwartkruis, 1999). In *Dictyostelium*, Rap1 is asymmetrically activated at the leading edge of migrating cells and controls dynamic regulation of cell adhesion and helps establish cell polarity by locally modulating myosin II assembly and disassembly through the Rap1/Phg2 signaling pathway(Jeon et al., 2007b; Lee and Jeon, 2012). Recently it has been demonstrated that the spatial and temporal regulation of Rap1 activity by Rap1 GAP proteins plays an important role in the control of cell adhesion and cell migration (Jeon et al., 2007a; Jeon et al., 2009; Mun et al., 2014).

RapGAP3, which mediates Rap1 activity regulation at the apical tip-forming stage of multicellular development, is rapidly translocated to the cell cortex in response to chemoattractant stimulation and is found preferentially at the anterior regions of migrating cells (Jeon et al., 2009). RapGAP3 contains three PH domains at the N-terminal, an actin binding I/LWEQ domain in the central region, and a GAP domain at the C-terminal. The localization of RapGAP3 is mediated by all of these three different

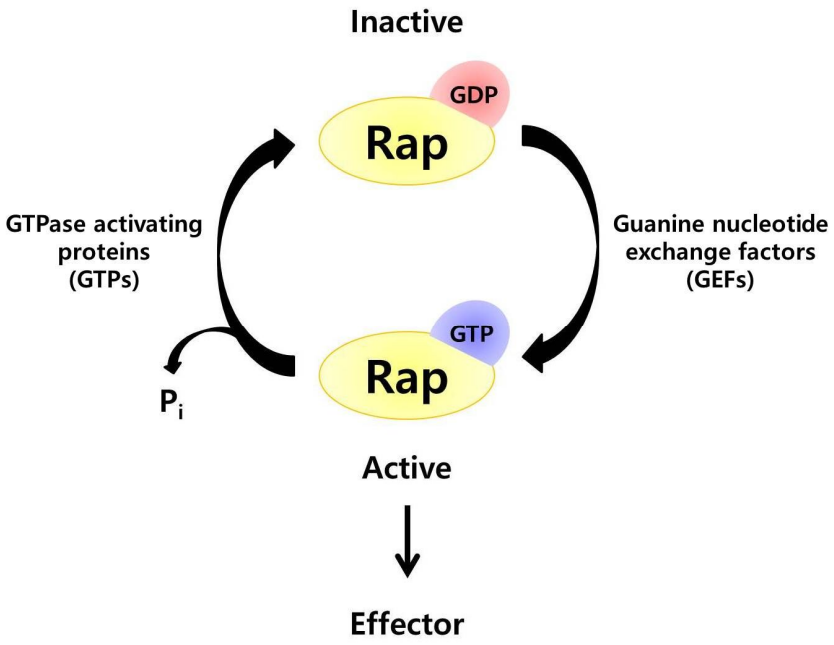

Figure 1. The GTPase cycle of Rap1.

Rap1 GTPase cycle is regulated an inactive GDP-bound state and an active GTP-bound state. The GTP-bounding Rap mediates signaling by connecting with and effector proteins (de Rooij et al., 1998).

domains (Lee et al., 2014). Interestingly, it was reported that the I/LWEQ domain in the central region of RapGAP3 was sufficient for posterior localization in migrating cells, as opposed to leading-edge localization of full-length RapGAP3, indicating that RapGAP3 contains all components for posterior and anterior localization in migrating cells (Lee et al., 2014). The I/LWEQ domain was originally identified on the basis of sequence similarity in several F-actin binding proteins (McCann and Craig, 1997). To understand the spatial mechanism that mediates anterior/posterior asymmetric localization of RapGAP3 during migration, here I further examined and compared the subcellular localizations of truncated RapGAP3 proteins and other F-actin binding proteins. These results show the minimal amino-acid sequence in the I/LWEQ domain of RapGAP3 required for anterior/posterior localization, and provide some important insights into asymmetric localization of the signaling molecules mediating cell migration in response to extracellular stimuli.

II. Materials and Methods

II-1. Cell culture, and strains

Dictyostelium KAx-3 cells were cultured axenically in HL5 medium at 22°C (Nellen et al., 1984). The HL5 medium contained 6 ml of 100 × antibiotic-antimycotic solution and 16 ml of 50% glucose per 600 ml. The expression plasmid of GFP-ABP (DictyBase ID #472, pDXA-GFPABD120) was obtained from the DictyBase Stock Center..

II-2. Plasmids

For expression of the truncated I/LWEQ domains of TalinA and RapGAP3 proteins, the regions in TalinA and RapGAP3 marked in the diagram (Fig. 3C and Fig. 4A) were amplified by PCR and cloned into the *Eco*RI-*Xho*I site and the *Bgl*II-*Xho*I site of a pEXP-4(+) GFP-expression vector, respectively (Jeon et al., 2009). The primers are summarized in Table 1. The expression plasmids for GFP-coronin, GFP-LD1 (#137) and GFP-RapGAP3 (#624) were described previously (Jeon et al., 2009; Lee et al., 2014).

For expression of GFP-RapGAP3(#624), the full coding sequence of *rapGAP3* cDNA was generated by RT-PCR, cloned into the *Bgl*II-*Xho*I site of pBluescript KS (−), sequenced, and subcloned into the GFP-expression. The plasmids were transformed into KAx-3 cells, and the cells were maintained in 10 μg/ml of G418.

Table 1. PCR primers used for truncated proteins of I/LWEQ domain in RapGAP3.

Gene (Acc. No.)	Name	Forward sequence (5′→3′)	Reverse sequence (3′→5′)	Location
rapGAP3 (DDB0229869)	#624-RapGAP3	ATGCATACAGGAGAATAC	TTATAAAAATTGAGAAATATAAT	1 – 1167 a.a
	#137-LD1	GGTGGTTTCAATAGTGGTG	TTATGTAGTTGAAATATTC	331 – 755 a.a
	#538-LD3	AATAATACAATAAGTTCAAG	TTATGTAGTTGAAATATTC	461 – 755 a.a
	#545-LD5	GATGGTGATGATTTAAAG	TTATGTAGTTGAAATATTC	487 – 755 a.a
	#546-LD6	GTTTTCACATTTCTTTTCTCTG	TTATGTAGTTGAAATATTC	528 – 755 a.a
	#581-LD10	GATGGTGATGATTTAAAG	TTATGGTGGTGTTATTAATTGATG	487 – 680 a.a
	#582-LD11	GATGGTGATGATTTAAAG	TTACTTACGATGATGGAAAATACC	487 – 604 a.a
	#610-LD12	GATGGTGATGATTTAAAG	TTATCTTGAATACTCAATAGG	487 – 647 a.a
	#180	GGTGGTTTCAATAGTGGTG	CTTTAAGAATTCCACTTCC	331 – 575 a.a
	#181	GGAAGTGGAATTCTTAAAG	TTATGTAGTTGAAATATTC	574 – 755 a.a
talinA (DDB0001399)	#598-TalFC	ATCTCTGATGCTGGTAAAGG	TTAATTTTTATTATAATTTTGTTTTC	2094 – 2492 a.a
	#555-TalFU	GAGGAAGATAACGTACTCGAAG	TTAATTTTTATTATAATTTTGTTTTC	2249 – 2492 a.a
	#556-TalFB1	GGTAAATTGGATGCTGAAGG	TTAATTTTTATTATAATTTTGTTTTC	2293 – 2492 a.a

Acc. No. indicates protein coding gene number of DictyBase.

II-3. Chemotaxis

As previously described (Lee et al., 2014), the subcellular localization of proteins in response to chemoattractant stimulation was examined. Vegetative cells were washed twice with Na/K phosphate buffer (pH 6.1) and were resuspended at a density of 5×10^6 cells/mL in Na/K phosphate buffer. Aggregation competent cells were prepared by pulsing the cells with 30 nM cAMP at 6 min intervals for 5 h. The pulsed cells were placed on glass-bottomed microwell plates. For imaging chemotaxing cells, a micropipette (FemtotipsII, Eppendorf Inc) filled with 150 μM cAMP was positioned near the cells for stimulation. Images of chemotaxing cells were taken at time-lapse intervals of 6 s for 30 min using an inverted microscope (IX71; Olympus, Japan) with a camera (DS-Fi1; Nikon, Japan).

II-4. Image acquisition

Quantitative analysis of membrane or cortical localization of GFP fusion proteins was performed as described previously (Jeon et al., 2007a; Sasaki et al., 2004). Aggregation competent cells were allowed to adhere to the plates for 10 min, and then were uniformly stimulated with 10 μM cAMP. Fluorescence images were taken at time-lapse intervals of 1 s for 1 min using a confocal microscope (DM IRE2; Leica) with HCX plan Apo NA 1.40 63 × objective lenses (oil CS; Leica) and a camera (EM-CCD; Hamamatsu Photonics). The frames were captured using NIS-elements software (Nikon) and analyzed using ImageJ software (National Institutes of Health, USA). The fluorescence intensity of the cell cortex was measured, and the level of cortical GFP-fusion proteins was calculated by dividing the intensity at each time point (Et) by the intensity before stimulation (Eo).

III. Results

III-1. The I/LWEQ domain in RapGAP3 required for posterior localization

RapGAP3 contains several domains, three PH domains at the N-terminal, an I/LWEQ domain in the central region, and a GAP domain at the C-terminal (Fig. 2A). It has been reported that the PH domains and the GAP domain are required for anterior localization of the protein in migrating cells while the I/LWEQ domain is for posterior localization (Jeon et al., 2009; Lee et al., 2014). The full-length RapGAP3 was highly accumulated at the anterior in migrating cells and a small amount of the protein was also found at the lateral and posterior regions (Fig. 2B). In contrast, highly accumulated GFP-fusion I/LWEQ domain of RapGAP3 (#137 GFP-LD1) was found at the posterior in migrating cells with a decreasing gradient from the rear to the front of cells. These data indicate that a single protein, RapGAP3, contains all components for both anterior and posterior localization of the protein in migrating cells, and the components for posterior localization are probably in a masked state in full-length RapGAP3 since the full-length RapGAP3 localizes to the leading edge of the cell.

When the cells were uniformly stimulated with chemoattractants, the full-length RapGAP3 exhibited rapid and transient translocation to the cell cortex, whereas the truncated, but still I/LWEQ domain-containing RapGAP3 protein showed no clear translocation (Fig. 2C). These results are in agreement with the fact that the signaling proteins accumulated at the anterior region in migrating cells show transient translocation to the cortex in response to uniform chemoattractant stimulation while the proteins at the posterior display no such clear translocation (Artemenko et al., 2014; Lee et al., 2014).

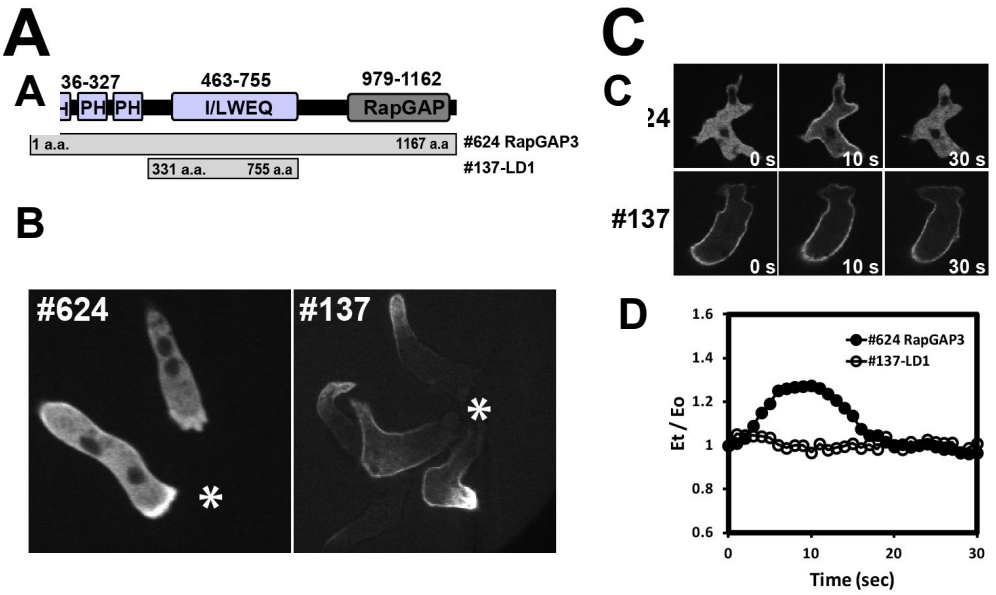

Figure 2. Localization of full-length RapGAP3 and the I/LWEQ domain of RapGAP3 in migrating cells.

(A) Domain structure of RapGAP3 and schematic diagram of truncated RapGAP3 proteins. (B) Localization of the fragments in chemotaxing cells. The asterisk indicates the position of micropipette emitting chemoattractant cAMP. (C) Translocation of the proteins to the cell cortex in response to uniform chemoattractant stimulation. Fluorescence images were taken after stimulating the cells with cAMP, and representative images at 0, 10, and 30 s after stimulation from time-lapse recordings are presented. (D) Translocation kinetics of the proteins to the cell cortex in response to chemoattractant stimulation. The graphs represent the mean values of data on several cells from at least two separate experiments. n = 80 and 78 cells for #624 RapGAP3 and #137-LD1, respectively.

III-2. Localization analysis of the I/LWEQ domain of TalinA in migrating cells

The I/LWEQ domain was originally identified in the analysis of several F-actin binding proteins including talin, HIP and Sla2p (McCann and Craig, 1997). The presence of the I/LWEQ domain in RapGAP3 was predicted by Block Maker analysis of RapGAP3 with *Dictyostelium* Talin A and B proteins. Even though there are slight differences in the distance among each block between RapGAP3 and talin proteins, RapGAP3 has a similar I/LWEQ domain to that of the talin proteins (Fig. 3A and B). To determine whether the I/LWEQ domain in TalinA shows a similar localization in migrating cells to RapGAP3, I prepared a series of truncated TalinA proteins containing the I/LWEQ domain and examined localizations of the proteins in migrating cells (Fig. 3C). It is known that the F-actin binding affinity of the TalinA I/LWEQ domain is regulated by intrasteric inhibition of an upstream α-helix region, which is located at around 50 amino-acids upstream of the first block within the I/LWEQ domain (Senetar et al., 2004). First, I examined two truncated talin proteins including the regulatory upstream α-helix region. The two truncated talin proteins were highly accumulated at the anterior region in migrating cells and were also found at the lateral and posterior regions, even though there was a slight difference between two proteins. In contrast, the truncated talin proteins containing only the region of I/LWEQ domain were found at the posterior but not the anterior regions (Fig. 3C), which is similar to that of the RapGAP3 I/LWEQ domain. Upon uniform chemoattractant stimulation, truncated talin proteins including the upstream regulatory region (GFP-TalFC and GFP-TalFU) showed transient translocation to the cell cortex, while the I/LWEQ domain only protein (GFP-TalFB1) displayed no clear translocation (Fig. 3D). These results indicate that the I/LWEQ domain in TalinA possesses posterior localization determinants, as in RapGAP3, in migrating cells.

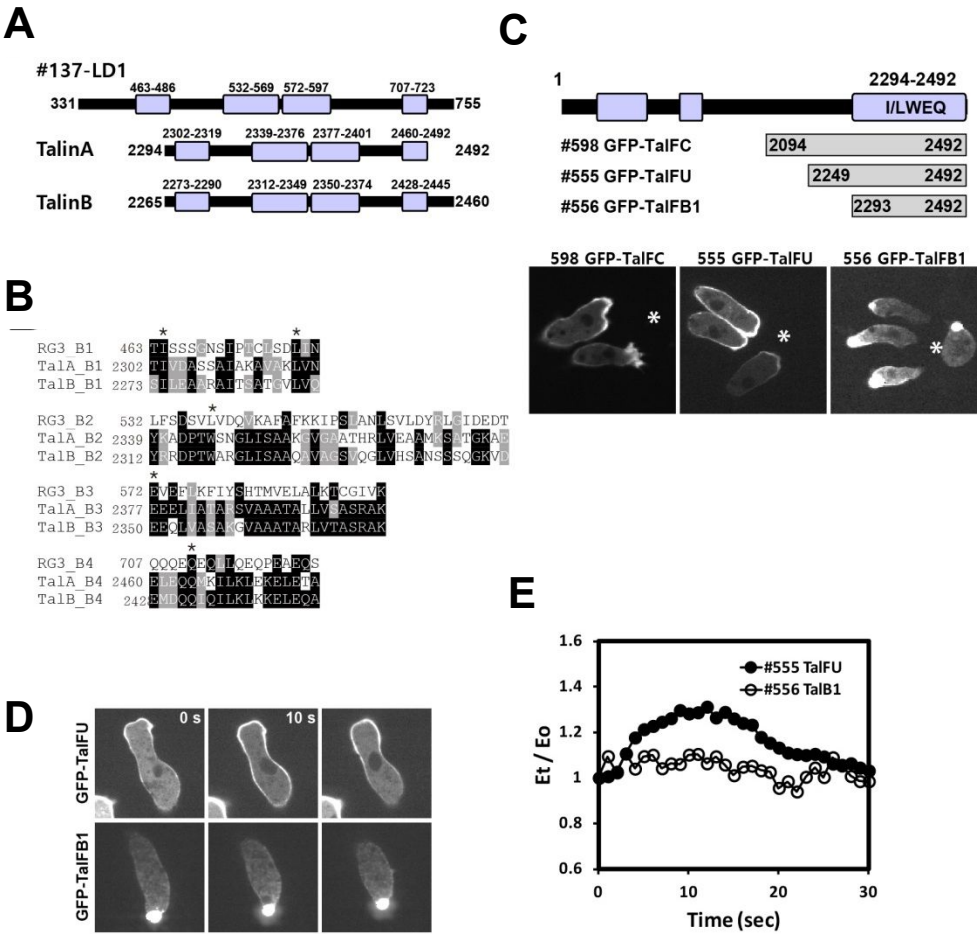

Figure 3. Localization of the I/LWEQ domain of TalinA in migrating cells.

(A) Block structures of the I/LWEQ domains in RapGAP3 and talin proteins. (B) Multiple alignment of amino acid sequences of the I/LWEQ domains. The asterisks indicate the amino acids conserved in the I/LWEQ domains. (C) Localization of the I/LWEQ domain of TalinA in migrating cells. The asterisk indicates the position of micropipette emitting chemoattractant cAMP. (D) Translocation of the proteins to the cell cortex in response to uniform chemoattractant stimulation. Representative fluorescence images at 0, 10, and 30 sec after stimulation from time-lapse recordings are presented. (E) Translocation kinetics of the proteins to the cell cortex in response to chemoattractant stimulation. Fluorescence intensity at the cell cortex was quantified and graphed as described in Figure 2. The graphs represent the mean values of data on several cells from at least two separate experiments. n = 72 and 36 cells for #555 GFP-TalFU and #556 GFP-TalFB, respectively.

III-3. Localization of truncated I/LWEQ domain proteins of RapGAP3 in migrating cells

To characterize minimal determinants of the I/LWEQ domain in RapGAP3 for asymmetrical posterior localization in migrating cells, I prepared a series of truncated GFP-fusion proteins of the I/LWEQ domain and examined the localizations of the proteins in migrating cells (Fig. 4). First, I determined the most N-terminal residues which are required for cell cortex localization. GFP-LD6 (528 - 755 a.a) was found in the cytosol while all other truncated proteins (LD3 and LD5) containing the same C-terminal region but longer N-terminal regions than LD6 were preferentially found at the posterior of migrating cells, suggesting that the amino acids at the N-terminal region of LD5 (487 - 755 a.a) are required for cell cortex localization. I examined the localization of the proteins which contain the same N-terminal as LD5 but further truncated C-terminals. GFP-LD10 (487 - 680 a.a) showed posterior localization in migrating cells almost to the same extent as LD5 (Fig. 4B). Surprisingly, GFP-LD11 (487 - 604 a.a), which was further truncated at the C-terminal relative to LD10, was observed at not only the posterior region but also the anterior and lateral sides of the cell. Additional truncated proteins that were further deleted from the C-terminal of LD11 were found in the cytosol (data not shown). These results suggest that the truncated RapGAP3 proteins LD10 and LD11 are at the borderline for minimal-size proteins in the posterior and cell cortex localization in migrating cells, respectively. Furthermore, these results indicate that the minimal region of RapGAP3 that is required for posterior localization in migrating cells also contains anterior localization components. Four α-helixes were predicted in the LD10 region of RapGAP3 (Fig. 4C). The fourth α-helix, which were predicted at 121 - 136 amino acids in the region of LD10, might be

important in mediating anterior/posterior localization of the proteins, since this structure was predicted to be present in the posterior localizing LD10 proteins but not the LD11 proteins which were observed at the posterior and anterior regions.

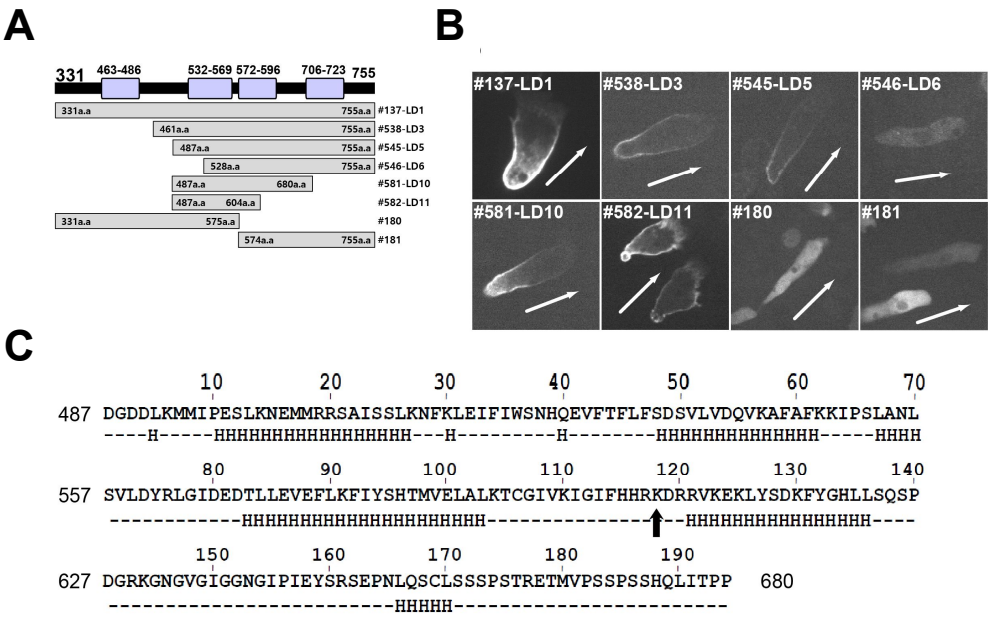

Figure 4. Localization of truncated I/LWEQ domain proteins of RapGAP3 in migrating cells.

(A) Diagram of truncated RapGAP3 proteins. (B) Localization of GFP-fusion truncated proteins in chemotaxing cells. The arrow indicates the direction of cell movement. (C) Secondary structure of LD10 RapGAP3 predicted at network protein sequence analysis at NPS@ server. H : α-helix. The arrow indicates the C-terminal of LD11.

III-4. Comparison of the localizations of GFP-LD10 and GFP-LD11 with F-actin binding proteins, Coronin and ABP

Previous reports suggested that posterior localization of the I/LWEQ domain of RapGAP3 is likely mediated by F-actins at the lateral and posterior regions of cells, which have different properties compared to the newly formed F-actin at the leading edge of migrating cells (Lee et al., 2014). To investigate the probability that GFP-LD10 and GFP-LD11 might have different affinities to distinct sets of actin filaments, I compared the localizations of the proteins in migrating cells with those of specific F-actin marker proteins, coronin and ABP-120, and examined the translocation kinetics of the proteins to the cell cortex in response to uniform chemoattractant stimulation (Fig. 5). GFP-LD10 was observed only at the posterior region in migrating cells with a decreasing gradient from the back to the front, whereas the further truncated LD11 was found at the posterior and the anterior protruding regions. The localization of GFP-LD11 was similar to that of GFP-ABP, but not GFP-Coronin. Coronin is a well-known F-actin binding protein, used as a maker protein for newly formed F-actin, physically associates with the Arp2/3 complex and inhibits actin nucleation activity of the complex (Cai et al., 2007; Chan et al., 2011; Jeon et al., 2007a). It was reported that the F-actin binding affinity of human coronin is approximately 50-fold higher for freshly polymerized actin compared with filaments polymerized from pure ADP-bound monomers (Cai et al., 2007). GFP-Coronin was mainly observed at the anterior region, indicating that new F-actin polymerization occurs at the protruding region of the cells. In contrast, another F-actin binding protein, ABP-120 was found at the anterior, lateral, and posterior regions. ABP-120 is one of the most abundant F-actin cross-linkers in *Dictyostelium* and contains an actin binding domain (ABD) at the N-terminal region. GFP-fusion proteins with the actin binding domain of ABP-120 were used for visualizing all sets of F-actins

at cell cortex, pseudopods, and filopods (Washington and Knecht, 2008).

All proteins in our study were found in the cytosol in the presence of latrunculin B, an inhibitor of F-actin polymerization, indicating that all proteins localize to the cell cortex in an F-actin dependent manner (Fig. 5C). Taken together, these results suggest that LD10 might have a strong binding affinity to pre-existing F-actins at the posterior while LD11 has affinity to not only the F-actins at the posterior but also the newly formed F-actins at the anterior of the cells.

III-5. Translocations of GFP-LD10 and GFP-LD11 to the cell cortex upon chemoattractant stimulation

The proteins which are located at the leading edge of migrating cells generally exhibit clear translocation to the cell cortex in response to uniform chemoattractant stimulation, whereas the proteins localized to the posterior in migrating cells display no translocation to the cortex (Artemenko et al., 2014; Lee and Jeon, 2012; Lee et al., 2014). As expected, the level of GFP-LD10, which localizes at the posterior in migrating cells, at the cortex was not changed upon uniform chemoattractant stimulation. In contrast, the level of GFP-LD11, which is accumulated at the anterior and the posterior regions in migrating cells, rapidly and transiently increased at the cortex with a peak at approximately 10 sec in response to chemoattractant stimulation, and then decreased to the basal level within 30 sec (Fig. 5D and E). The two F-actin binding maker proteins showed slightly different translocation kinetics to the cell cortex in response to chemoattractant stimulation. The majority of GFP-Coronin was found in the cytosol before stimulation. Upon chemoattractant stimulation, GFP-Coronin was translocated to the cortex with a peak at 10 - 15 sec, which is slightly delayed compared to previously reported data (Etzrodt et al., 2006; Jeon et al., 2007a), and the level of the protein decreased to the basal level within 30 sec. The level of GFP-ABP at the cortex was more rapidly increased, compared to GFP-Coronin and GFP-LD11, with a peak at 5 - 7 sec, and then decreased to the basal level within 20 sec. The initial translocation kinetics of GFP-LD11 was similar to that of GFP-ABP but the delocalization kinetics of the protein at the cortex was similar to that of GFP-Coronin (Fig. 5E), suggesting that LD11 has a partially overlapping F-actin binding property with the two actin binding proteins, ABP-120 and Coronin.

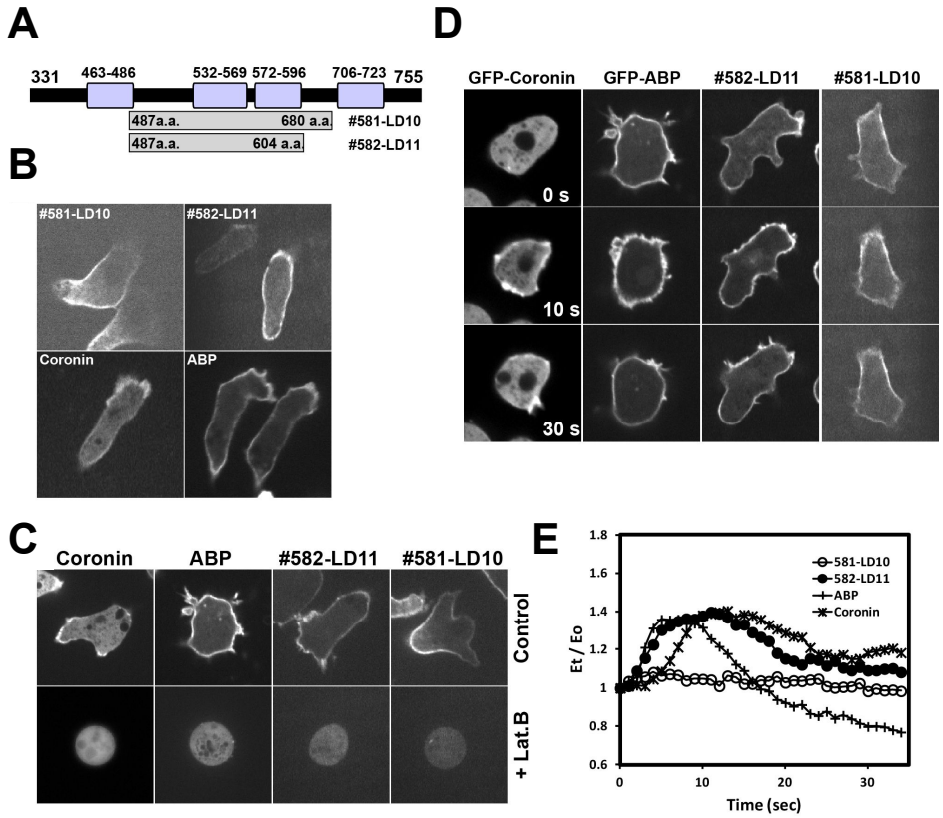

Figure 5. Comparison of localizations of GFP-LD10 and GFP-LD11 with GFP-Coronin and ABP.

(A) Diagram of GFP-LD10 and GFP-LD11. (B) Localization of GFP-LD10, GFP-LD11, GFP-Coronin and GFP-ABP in migrating cells. (C) Localization of the proteins in the presence of Lat. B. (D) Translocation of the proteins to the cell cortex upon chemoattractant stimulation. Three representative fluorescence images at 0, 10, 30 s after stimulation are presented. (E) Translocation kinetics of the proteins to the cell cortex in response to chemoattractant stimulation. Fluorescence intensity at the cell cortex was quantified and graphed as described in Figure 2. The graphs represent the mean values of data on several cells from at least two separate experiments. n = 46, 86, 44, and 52 cells for #581-LD10, #582-LD11, ABP, and Coronin, respectively.

IV. Discussion

Cell polarity formation upon extracellular stimulation is required for directed cell migration and is mediated by asymmetrical localization or activation of the signaling molecules in the cell (Artemenko et al., 2014; Kortholt and van Haastert, 2008; Lee and Jeon, 2012). Here I determined the minimally required amino acids in the I/LWEQ domain of RapGAP3 that enables posterior localization in migrating cells. More importantly, I found that the minimal region of the protein required for posterior localization (LD10; Fig. 4) could localize to the anterior with some additional deletion of its C-terminal (LD11), indicating that the same F-actin binding domain can be modulated to localize to the anterior or posterior of the cell through small protein fragments. These results suggest that anterior or posterior localization of the F-actin binding domain in RapGAP3 is likely dependent upon structural and biochemical properties of F-actins at the cell cortex.

The I/LWEQ domain was originally identified as an actin-binding motif in several actin binding proteins such as talins, HIPs, and Slap Proteins (McCann and Craig, 1997; Senetar et al., 2004). The I/LWEQ domain in RapGAP3 comprises around 425 amino acids forming four conserved blocks even though it is much longer than others of *Dictyostelium* TalinA and TalinB. The I/LWEQ domain of RapGAP3 is sufficient for posterior localization in the cell. In agreement with our prior results (Lee et al., 2014) (Fig. 2), GFP-fusion proteins containing the I/LWEQ domain of *Dictyostelium* TalinA localized to the posterior region of migrating cells, suggesting that the posterior localization of the I/LWEQ domain might be general to other actin-binding proteins containing this motif. However, there appear to be some differences in the deterministic components for asymmetric localization of the protein between RapGAP3 and TalinA. It is known that the F-actin binding affinity of the TalinA I/LWEQ domain is regulated by

intrasteric inhibition of an upstream α-helix, which is located at approximately 50 amino-acids upstream of the first block within the I/LWEQ domain (Senetar et al., 2004). These results demonstrate that block 2 and block 3 of the four blocks, from 487 a.a to 604 a.a (LD11; Fig. 4) in RapGAP3, are essential for localization at the cell cortex including the anterior in an F-actin dependent manner. Instead, the 70 amino acids between block 3 and block 4 are critical for posterior localization in migrating cells. Four α-helixes were predicted in the minimal region for posterior localization and the last α-helix, which is present in the posterior localizing proteins but not the anterior localizing proteins i.e., LD11, might play some important roles in localizing the proteins to the posterior or other specific sites in the cell, as the upstream α-helix is involved in the regulation of the F-actin binding affinity (Senetar et al., 2004) and the localization of the I/LWEQ domain in TalinA.

Actin filaments in the cell are organized into several different forms and functional arrays by various actin-binding proteins, resulting in F-actins with different biochemical and structural properties (Galkin et al., 2010; Shimozawa and Ishiwata, 2009; Uyeda et al., 2011). A newly formed F-actin at the front of migrating cells provides the mechanical force for membrane protrusion, and another type of F-actin is required for contraction of the cell body by interacting with myosin II at the posterior and lateral sides of the cell (Artemenko et al., 2014; Lee and Jeon, 2012; Ridley et al., 2003). It has been previously proposed that the I/LWEQ domain of RapGAP3 might bind to only the pre-existing F-actin at the rear and lateral sides of the cell but not the newly formed F-actin at the front in migrating cells, leading to localization to the posterior and lateral sides of the cell (Lee et al., 2014). The present study further characterized the minimal protein fragments required for posterior or anterior localization of the I/LWEQ domain of RapGAP3. The localization and translocation kinetics to the cell cortex of GFP-LD11, which is the minimal size protein required for localization at the cell cortex including the

anterior, in response to chemoattractant stimulation was similar to that of GFP-ABP, which is an F-actin binding and cross-linking protein and observed at all cell cortexes including the anterior and the lateral and posterior of migrating cells(Washington and Knecht, 2008). Another F-actin binding protein Coronin, which was used as a marker protein for a newly formed F-actin (Chan et al., 2011; Jeon et al., 2007a; Jeon et al., 2009), showed high accumulation at the front of migrating cells and rapid and transient translocation to the cell cortex in response to chemoattractant stimulation, indicating that new polymerization of F-actin occurs at the anterior region of migrating cells. Our results support the suggestion that the minimal protein fragment for anterior localization (LD11) is likely to bind to both newly formed and pre-existing F-actins, leading to localization to the cell cortex including the anterior, lateral, and posterior regions of the cell. On the other hand, the minimal fragment for posterior localization (LD10) might bind to only pre-existing F-actins and are excluded from the anterior, i.e., the newly formed F-actins, and is directed to localize to the cortex at the posterior and lateral sides of the cell. Two types of F-actins with different biochemical and structural properties-one is a cross-linked and newly formed F-actin at the front and the other is a stretched F-actin at the rear and lateral sides of the cell-appear to be key factors for determining the localization of the actin-binding proteins to specific sites of the cell; a structural polymorphism in F-actin has been demonstrated in many reports (Galkin et al., 2010). Electron cryomicroscopy showed that frozen, hydrated actin filaments contained a multiplicity of different structural states, with variable twist as well as a variable tilt of subunits (Galkin et al., 2002). F-actin properties are modulated by over 150 different actin binding proteins, resulting in functionally distinct regions of the cytoskeleton (Salwinski et al., 2004). It has been shown that a myosin II domain, which localizes to the posterior of a migrating cell, preferentially binds to stretched actin filaments in the rear cortex and cleavage furrows (Uyeda et al., 2011). In addition, at the leading edge,

actin is assembled as a dendritic network forming a lamellipodial shape(Ridley et al., 2003). The present study suggests that the minimally required regions for anterior/posterior localization in the I/LWEQ domain of RapGAP3 might have preferential binding affinities for stretched, pre-existing F-actin at the rear and lateral sides of the cell or cross-linked, newly formed F-actin at the front of the cell. However, there might be another possibility that the posterior localization of the proteins might be attributed to the transport of the proteins by a retrograde actin flow (Maiuri et al., 2015; Weber et al., 2002). This study contributes to understanding the mechanisms that direct asymmetrical distribution of the signaling molecules in response to extracelluar stimuli and the establishment of cell polarity by locally modulating Rap1 activity.

PART II. Study on Fucoidan-Mediated Cell Polarization in Osteoblasts

I. Introduction

Fucoidan is a sulfated polysaccharide found in the extracellular matrix of brown algae including *Undaria pinnatifida*, *Fucus vesiculosus* and *Ecklonia cava* and contains a large proportion of L-fucose and sulfate (Senthilkumar and Kim, 2014; Senthilkumar et al., 2013). Fucoidan has been reported to possess diverse biological activities including anti-viral, anti-bacterial, anti-inflammatory, anti-coagulant, anti-oxidant, anti-angiogenic effects, and antitumor activities (Durig et al., 1997; Lee et al., 2012; Nakamura et al., 2006; Senthilkumar and Kim, 2014; Senthilkumar et al., 2013; Wang et al., 2010; Xue et al., 2013; Zapopozhets et al., 1995). The anti-cancer activities of fucoidan have been demonstrated in many different types of cancers such as breast cancer, adenocarcinoma, and colon cancer by arresting the cell cycle and inducing apoptosis (Boo et al., 2013; Park et al., 2013; Senthilkumar et al., 2013; Yang et al., 2013). Recently, fucoidan extracted from marine brown algae *U. pinnatifida* was found to induce the differentiation and mineralization of osteoblastic cells (Changotade et al., 2008; Cho et al., 2009; Jeong et al., 2013; Park et al., 2012). Fucoidan treatment resulted in increased expression of osteogenesis-specific marker genes in human adipose-derived stem cells (Park et al., 2012). Furthermore, the activity of alkaline phosphatase and level of osteocalcin, a phenotypic marker of early-stage osteoblastic differentiation, were increased in osteoblastic cells treated with fucoidan (Cho et al., 2009). In addition, the fucoidan has recently been used as an additive to biomaterial-based scaffolds that

enhance bone reconstruction (Cho et al., 2009; Jeong et al., 2013). These data raised the possibility that fucoidan might be a potential candidate as an additive for biomaterial-based scaffolds to promote bone regeneration and could possibly be used in bone health supplements.

Bone reconstruction and repair require osteogenic cells to be recruited to the sites that need to be rebuilt. Failure of recruitment of the osteoblasts to the sites in need of bone formation may result in impaired fracture repair. Modulating the migration of the cells could offer opportunities to treat osteoporosis and fracture repair and improve bone regeneration (Dirckx et al., 2013; Meng and Xie, 2014; Nakahama, 2010; Pignolo and Kassem, 2011; Song and Park, 2014). Cell migration is a dynamic process that requires the coordinated regulation of adhesion and rearrangement of the cytoskeleton. The effect of fucoidan on cell migration has been tested in several types of cancer cells, and controversial results have been reported. In fucoidan-treated bladder cancer cells of human lung cancer cells, cell growth and migration were inhibited by activation of Akt signaling (Cho et al., 2014; Lee et al., 2012), whereas in canine peripheral polymorphonuclear cells, chemotaxis and actin polymerization were increased by fucoidan treatment (Kim et al., 2013).

Even though many studies have described the pharmacological properties of fucoidan in several different types of cells, and shown that it promotes osteoblastic cell differentiation, the effects of fucoidan on the cytoskeleton and migration of osteoblastic cells have not yet been studied. This study investigated the effects of fucoidan on the migration, morphology, and cytoskeleton of MC3T3 preosteoblastic cells and on cell growth and morphology of MG-63 human osteosarcoma cells.

II. Materials and Methods

II-1. Materials and Cell culture

Fucoidan purified from sporophyll of *Undaria pinnatifida* was obtained from HAERIM FUCOIDAN Co. (Wando, Korea). According to the manufacturer's information, the average molecular weight of fucoidan is 130 kDa, and it contains 21 ± 3% fucose, 20 ± 5% galactose, 2 ± 2% mannose, 30 ± 3% sulfate. All antibodies were purchased from Santa Cruz Biotechnology Inc (Santa Cruz, CA, USA). Transwell migration kits and TRITC conjugated-phalloidins were purchased from Corning Costar (Cambridge, MA, USA) and Sigma-Aldrich Inc (St Louis, MO, USA), respectively. β-actin antibody was purchased from Santa Cruz Biotechnology Inc (Santa Cruz, CA, USA). FITC Annexin V/PI apoptosis detection kit and TRITC conjugated-phalloidin were purchased from Life technologies Inc (Eugene, Oregon, USA) and Sigma-Aldrich Inc (St Louis, MO, USA), respectively. Dulbecco's Modified Eagle's Medium (DMEM), 100 × penicillin/streptomycin (p/s), and fetal bovine serum (FBS) were obtained from WELGENE Inc (Daegu, Korea). MC3T3-E1 and MG-63 osteoblastic cells were cultured in DMEM supplemented with 10% heat-inactivated FBS and 1% p/s at 37℃ in a concentration of 5% CO_2 gas. The culture medium was changed every 2 or 3 days. Every experiment was performed after cell starvation in serum-free media (SFM) containing 2% FBS for 12 h.

II-2. Cell viability assay

Cell viability was measured by 3-(4,5-Dimethylthiazol-2-yl)-2,5-diphenyltetrazolium bromide (MTT) assay as described previously (Cho et al., 2009). In brief, the cells (5×10^4 cells/well) were seeded and treated with various concentrations of fucoidan for 12 h or 24 h, followed by removing the media and then incubating with 0.5 mg/mL of MTT solution. After incubation for 3 h at 37℃ and 5% CO_2, the supernatant was removed, and the amount of formed formazan was measured at 560 nm using a microplate reader.

II-3. Wound healing assay

Wound healing assay was performed using 6-well plates as previously described (Lee et al., 2012). The amount of 2×10^6 MC3T3-E1 preosteoblastic cells were placed and incubated in 6-well plates containing media supplemented with 2% FBS for 12 h. After aspirating the medium, cells were scratched with a micropipette tip followed by washing with PBS. The rinsed cells were treated with fucoidan and incubated for 48 h. Cell migration into the wound area was photographed at the stages of 0 h, 12 h, 24 h, and 48 h. The level of cell migration was estimated by measuring the wound closure area using ImageJ software (NIH, Bethesda, MD, USA) and expressed as a percentage of the wound closure area to the original wound area at 0 h.

II-4. Transwell migration assay

Transwell migration assay using a 24-well Transwell unit with polycarbonate filters was performed as described in the instructions (Corning Costar). MC3T3-E1 cells were starved in a serum-free media for 12 h and then resuspended at a density of 5×10^5 cells/mL in serum-free media. Harvested cells (5×10^4 cells/well) were added to the upper part of the transwell plate containing fucoidan, and the lower compartment was filled with 10% FBS-containing media. After 48 h incubation, the non-migrated cells were removed from the upper surface of the filter membrane. The migrated cells on the lower surface of the filter were fixed in 100% methanol for 3 min, stained with Coomassie blue for 20 min, and imaged using a light microscope and NIS elements software. The amount of migrated cells was estimated as the percentage of migrated cells relative to control cells. The amount of control cells in 10% FBS-containing media in the lower container was set to 100% and the others are relative amounts.

II-5. Scanning Electron Microscopy

Scanning electron microscopic observation was performed using fucoidan-treated cells which were attached to the cover glasses. Cells on cover glasses were fixed with 2.5% glutaraldehyde in PBS at room temperature overnight, and then dehydrated in a graded series of ethanol. Air dried samples were coated with a supercritical point sputter-coated with SP 21030 for 60 sec and examined with a Hitachi S-4800 scanning electron microscope.

II-6. Cell adhesion and spreading assay

Adhesion and spreading assays were performed by a slightly modified method of Kucik (Kucik and Wu, 2005). 80% - 90% confluent cells which were fully attached on plates were washed with PBS and then incubated in media containing 2% FBS and 100 μg/mL of fucoidan for 12 h. Fucoidan-treated cells were harvested with 0.6 mM EDTA and resuspended at a density of 4×10^5 cells/mL in the same media. The amount of 1×10^5 cells were placed onto 24-well plates. After 1 h incubation, the cells on plates were photographed for counting the number of total cells, and unattached cells were removed by washing twice with PBS. Attached cells on plates were photographed and counted. Adhesion and spreading cells were presented as a percentage of attached and spread cells to total cells.

II-7. F-actin cytoskeleton staining

Cells were fixed with 3.7% formaldehyde in PBS for 5 min, followed by permeabilizing with 0.1% Triton X-100 for 1 min, and blocked with 1% BSA in PBS for 1 h. The cells were stained with Hoechst dye (4 μg/ml) and TRITC-phalloidin (Sigma-Aldrich) for nuclei and F-actin, respectively, at room temperature for 20 min. Stained cells were observed in Fluoreomount-G (SouthernBiotech, Birmingham, AL, USA) mounting solutions using an inverted microscope (IX71; Olympus, Tokyo, Japan) with a camera (DS-Fi1; Nikon, Tokyo, Japan).

II-8. Cytoskeletal fraction analysis

Immunoblotting for cytoskeletal fractions of F-actin were performed as described previously with a slight modification (Jeon et al., 2007b). Growing cells on plates were lysed by adding 1 mL of lysis buffer (20 mM TES at pH 6.8, 1% Triton X-100, 2 mM $MgCl_2$, 5 mM EGTA, 5 μg/mL Aprotinin, and 5 μg/mL Leupeptin) after aspirating the media, and the cytoskeleton fractions were isolated by centrifugation of the lysates at 4℃ for 10 min. The pellets were washed once with lysis buffer and then subjected to immunoblotting analyses with β-actin antibodies.

II-9. Cell growth rate assay

MG-63 cell growth rates were assessed using an in vitro growth assay. Cells were plated into 24-well plates containing culture medium with fucoidan at a density of 10,000 cells per well and were incubated for 7 days without changing media. Every 24 h, pictures of the plates were taken randomly, and the cells on the pictures were counted. The growth rate was calculated as the ratio of the number of the cells to the control.

II-10. Hoechst 33258 staining

Fucoidan-treated cells were stained with Hoechst 33258 (4 μg/ml) for 30 min at room temperature. The cells were washed twice with PBS, and the fragmentation of DNAs in nuclei was observed by an inverted fluorescent microscope (IX71; Olympus, Tokyo, Japan) with a camera (DS-Fi1; Nikon, Tokyo, Japan).

II-11. Annexin V/PI staining

Apoptosis of the cells were measured by using an Alexa Fluor® 488 Annexin V/Dead Cell Apoptosis Kit (Molecular Probes, Life technologies). The cells were seeded in 24-well plates and treated with various concentrations of fucoidan for 12 h. After washing the cells with PBS, annexin V and propidium iodide (PI) solution were added and incubated at room temperature for 15 min. Immediately after incubation, the cells were photographed by using an inverted fluorescent microscope, and the stained cells were counted. The apoptotic cells were presented as a percentage of annexin-stained cells to total cells.

II-12. Statistical analysis

The results were expressed as the mean ± standard deviation (SD) or standard error of measurement (SEM). Data were collected from at least three independent experiments and analyzed using Student's two-tailed t-test. *p<0.05 and **p<0.01 was considered statistically significant.

III. Results

III-1. Effects of fucoidan on migration in osteoblasts

MC3T3-E1 preosteoblastic cells were treated with several different concentrations of fucoidan after they were stably attached and starved in media containing 2% FBS for 12 h, and the cells were then scratched with a micropipette tip and imaged at the indicated times. A small amount of cells moved to the center 12 h after scratching. After 24 h, the scratched regions were partially filled with cells and they were completely filled after 48 h (Fig. 1A). Quantification of migration at the indicated times after scratching showed that the migration of the cells were decreased in the presence of fucoidan (Fig. 1B).

To examine whether the decrease of migration by fucoidan treatment might result from the reduction of viability, I measured cell viabilities by MTT assay (Fig. 1C). When the cells were treated with fucoidan, there was no statistically significant decrease in cell viability compared with that of the control cells, and only high concentration (400 μg/mL) of fucoidan showed a decrease of cell viability.

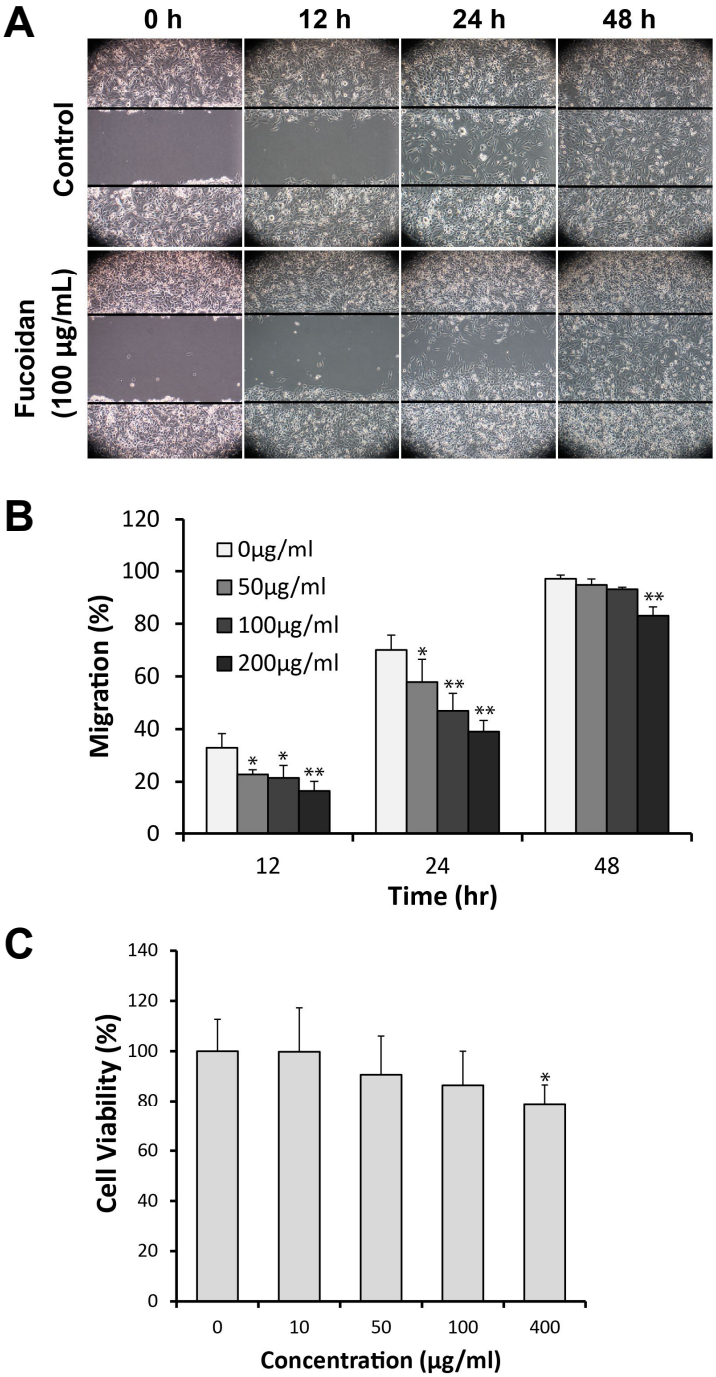

Figure 1. Effect of fucoidan on migration of stably attached osteoblasts

(A) Examination of migration by a wound-healing assay. Stably attached cells on the plates were treated with 100 μg/mL of fucoidan for 12 h, and the cells were then scratched with a pipette tip and imaged at the indicated times. (B) Quantification of migration. The level of cell migration was estimated by measuring the area of the wound at the indicated time using ImageJ software and expressed as percentages of the wound area relative to that at 0 h. The data shown are the means ± SD of three experiments (*p<0.05 and **p<0.01 compared to the control). (C) Cell viability assay. Cells were treated with various concentration of fucoidan for 24 h. The data shown are the means ± SD of three experiments (*p<0.05 compared to the control).

To confirm the effects of fucoidan on osteoblast migration, I examined migration of preosteoblastic cells in the presence of fucoidan using a transwell migration assay. Two containers are used in a transwell migration assay. Starved cells are placed in the upper compartment and chemoattractants are added in the lower compartment. The media containing 10% FBS were used as a chemoattractant in the lower container. Interestingly fucoidan-treated cells showed increased migration compared to control cells (Fig. 2A and B), contrary to the results of the previous wound healing assay. The number of the cells moved from the upper container to the lower container significantly increased in the presence of 50 μg/mL or 100 μg/mL of fucoidan, and the level of migration of the cells decreased to the basal in 200 μg/mL of fucoidan. The increased migration appears to result from the different conditions in which the cells were treated with fucoidan.

To determine how the conditions under which cells are treated with fucoidan affects migration, I conducted a wound healing assay in which conditions were more similar to the transwell migration assay. Harvested osteoblast cells, instead of stably attached cells used in the previous wound healing assay, were placed onto plates containing fucoidan and then incubated for 12 h followed by scratching with a micropipette tip as in the previous wound healing assay (Fig. 2C). The control cells in the media without fucoidan exhibited patterns of migration similar to those in the previous wound healing assay. The control cells seemed strongly attached to the plates, and the wound was completely filled with the cells within 48 h (Fig. 2C, upper panel). On the other hand, the cells treated with fucoidan were detached, floated after scratching, and the clear wound was not even formed (Fig. 2C, Lower panel).

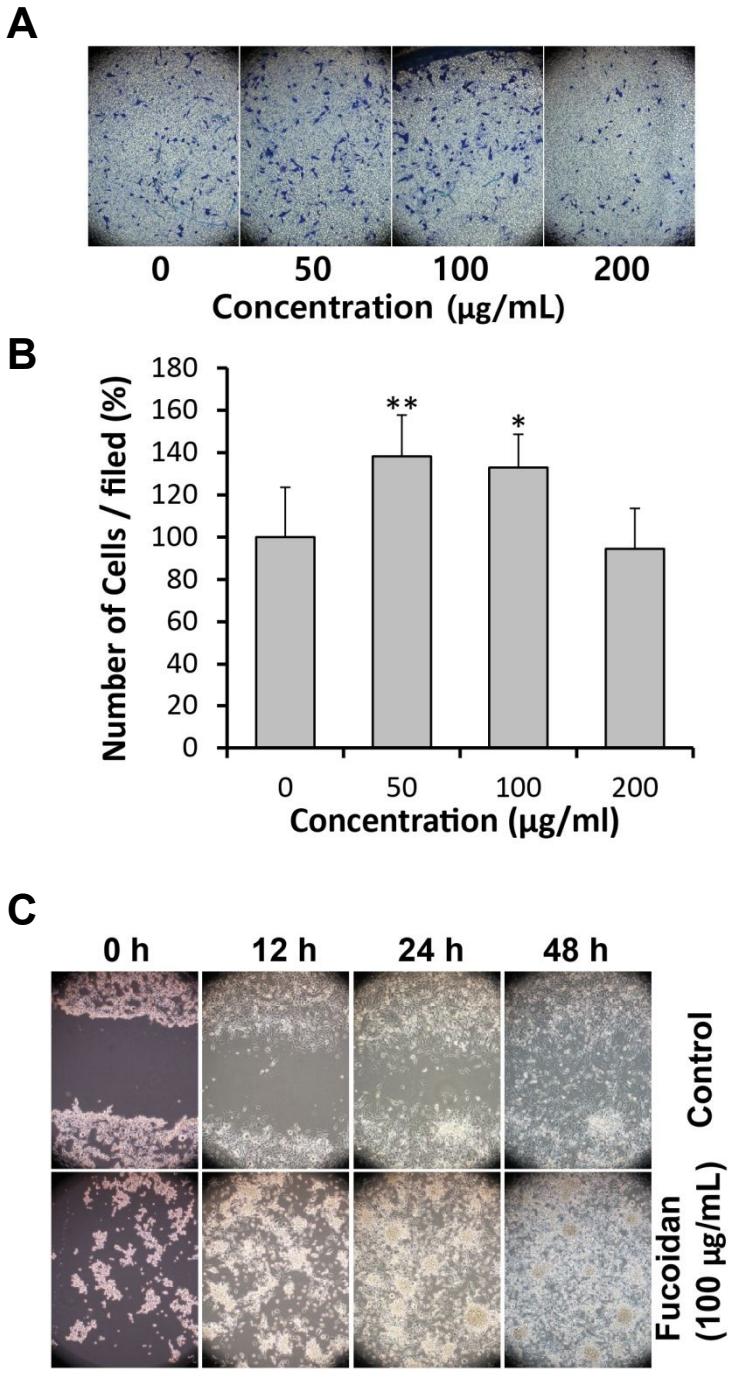

Figure 2. Migration of the cells treated with fucoidan before stable attachment

(A) Transwell migration assay. Starved cells in DMEM media containing 0% FBS for 12 h were harvested and placed in the upper chamber, followed by 24 h incubation in the presence of various concentration of fucoidan. In the lower container, Media containing 10% FBS were used as chemoattractants for migration of the starved cells. The migrated cells on the lower surface of the membrane in the upper container were visualized by Coomassie blue staining and observed under microscope. (B) Quantification of the migrated cells. The stained cells on the lower surface of the membrane were counted and expressed as percentages of migrated cells relative to control cells. The values are the means ± SD of three experiments (*p<0.05 and **p<0.01 compared to the control). (C) Wound healing assay. Harvested cells instead of stably attached cells were seeded and incubated in the presence of fucoidan for 12 h, and then the plates were scratched as in figure 1A.

III-2. Effects of fucoidan on cell morphology and rearrangement of the cytoskeleton

To investigate the effects of fucoidan on osteoblastic cells in detail, I examined changes in cell morphology after cells were treated with fucoidan. Fully grown cells were harvested and then placed on plates in the presence or absence of fucoidan as in the previous transwell migration assay, in which fucoidan-treated cells displayed increased migration. In the media without fucoidan, the cells became spread and developed thin protrusions within 4 h of incubation. In the presence of fucoidan, the cells were rounded at 1h of incubation after seeding on the plates and almost all of the cells exhibited similar rounded shapes even after 4 and 12 h of incubation, whereas the control cells displayed spreading after 4 h after seeding (Fig. 3A). Some aggregates of cells were found after 4 h after seeding in the presence of fucoidan. The images of scanning electron microscopy of the cells after 12 h incubation clearly showed that the cells that were in the presence of fucoidan were more rounded and aggregated than the control cells (Fig. 3B).

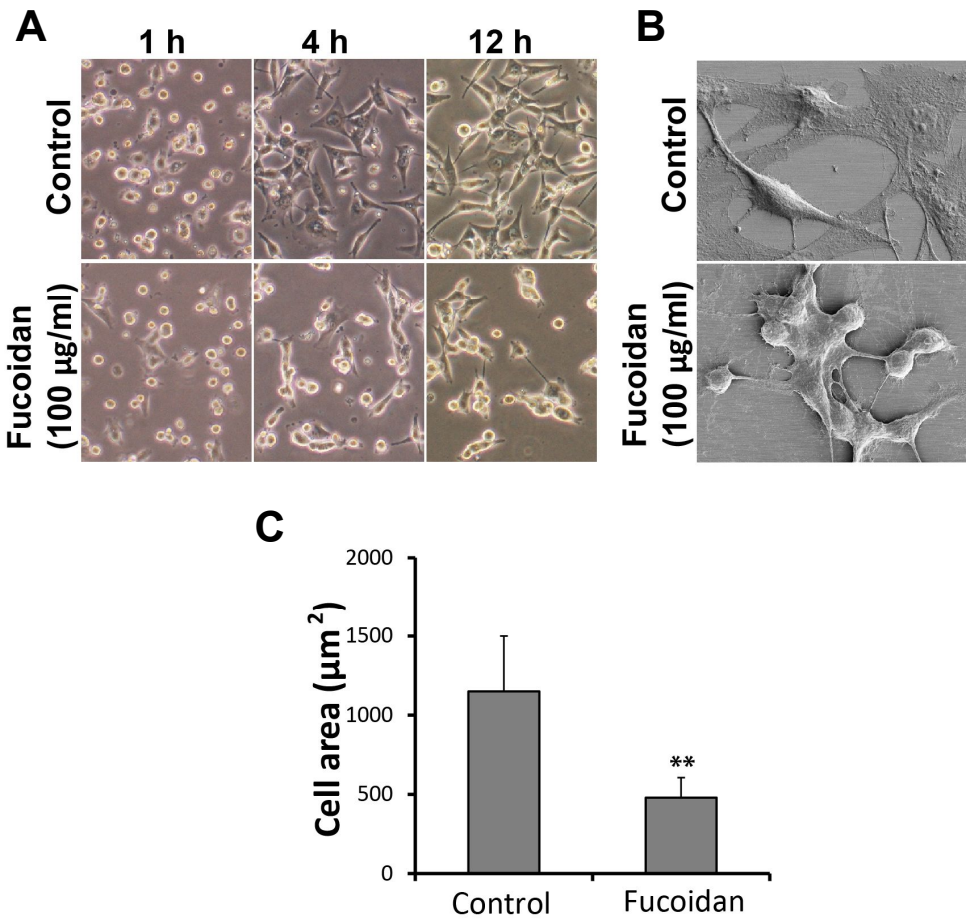

Figure 3. Morphology of the cells in the presence of fucoidan

(A) Morphology of the cells in the presence of fucoidan. Fully grown cells were harvested and placed on plates in the presence of fucoidan, and images were taken at the indicated times. (B) Scanning Electron Microscopy. After treating the cells with fucoidan for 12 h, images were taken. (C) The size of the cells treated with fucoidan for 12 h was quantified and graphed. The values are the means ± SD of three experiments (**p<0.01 compared to the control).

Next, I examined the effects of fucoidan on adhesion and spreading of osteoblasts (Fig. 4). Regardless of the conditions in which the cells were treated with fucoidan, all fucoidan-treated cells showed week adhesion compared to control cells. Adhesion decreased more when harvested cells were treated with fucoidan relative to when fully attached cells were used. The effects of fucoidan on cell spreading were similar to those on adhesion. These results suggest that fucoidan prevents adhesion and spreading of osteoblasts, and that the effects of fucoidan increase when cells are treated before they stabilize on the plates.

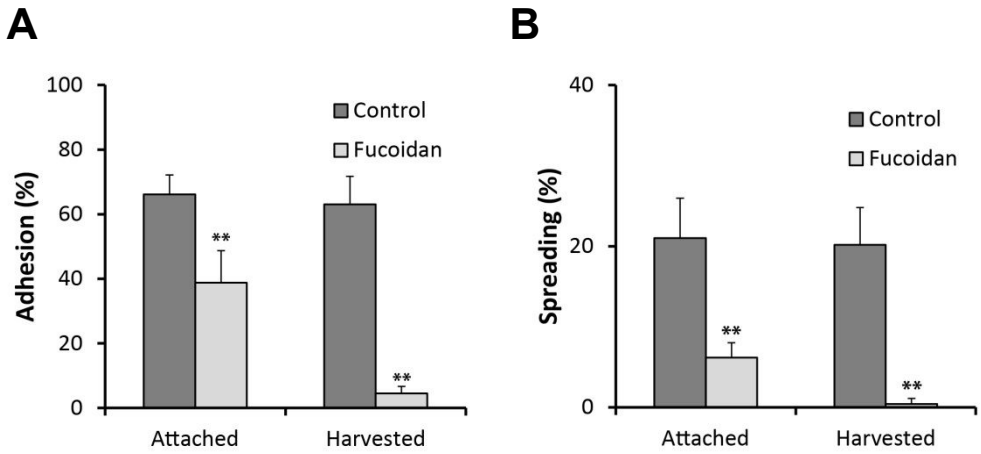

Figure 4. Adhesion and spreading of the cells in the presence of fucoidan

(A) Adhesion and (B) spreading of fucoidan-treated cells. Fully attached cells were treated with fucoidan for 12 h, and then harvested and used in the adhesion and spreading assay (Attached). Harvested cells, instead of stably attached cells, were treated with fucoidan on seeding and incubated for 12 h, and then used in the assay (Harvested). The values are the means ± SD of three experiments (**p<0.01 compared to the control).

Morphology and adhesion of cells are regulated by the cytoskeleton. To investigate the effects of fucoidan on the cytoskeleton, I examined the localization of F-actin with phalloidin staining. Harvested cells treated with fucoidan for 12 h were fixed and then stained by phalloidin (Fig. 5). As in the previous experiments, the cells were spread out and flat in the absence of fucoidan, and F-actin was stretched and relatively evenly distributed in a cell. On the other hand, the cells treated with fucoidan exhibited rounded and highly accumulated F-actin at the cell cortex.

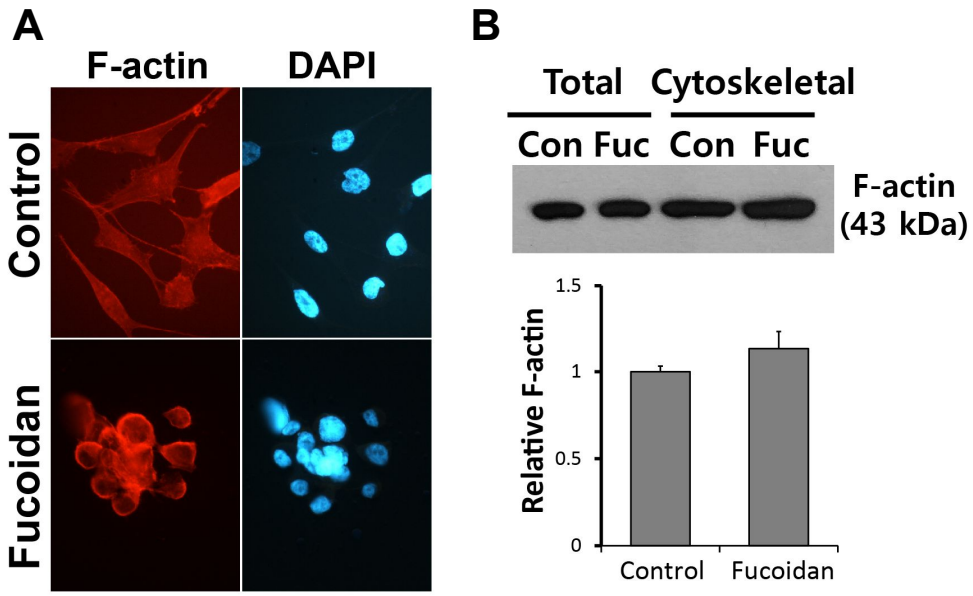

Figure 5. Localization of F-actin in fucoidan-treated cells

(A) F-actin and nuclei staining. F-actin and nuclei in fucoidan-treated cells were stained with TRITC-conjugated phalloidin and Hoechst dyes, respectively. (B) Quantification of F-actin. Cytoskeleton fractions were extracted and then immunoblotted with β-actin antibodies. Densities of the bands were quantified and graphed.

III-3. Fucoidan inhibits cell proliferation of MG-63 cells

A previous study showed that the effects of fucoidan on the migration of osteoblasts varied depending on the conditions under which the cells were treated. When the cells were treated with fucoidan upon seeding after harvest but not after stable attachment to the plates, the effects of fucoidan on the cells was more obvious. To increase the possibility of observing the effects of fucoidan, osteosarcoma MG-63 cells were treated with fucoidan upon seeding and then the cells were incubated for 12 or 24 h in all experiments.

I first determined the effect of fucoidan on the proliferation of MG-63 cells using the MTT assay. Harvested cells were incubated for 12 h in the presence of various concentrations of fucoidan. A statistically significant decrease in cell viability was observed in the presence of more than 50 μg/mL of fucoidan (Fig. 6A). In the presence of 200 μg/mL of fucoidan, cell viability was decreased to approximately 80% relative to the control. To confirm the effect of fucoidan on cell viability, I tested the growth rate of the cells in the presence of fucoidan for 7 days (Fig. 6B). The number of control cells in the absence of fucoidan gradually increased to approximately 12-fold of the original number of cells after 7-days of incubation. Compared to the control, MG-63 cells grew more slowly beginning at 4-days of incubation in the presence of fucoidan and the growth was considerable after 6 - 7 days of incubation in 100 - 200 μg/mL of fucoidan. The number of cells treated with 100 - 200 μg/mL of fucoidan after 7-days of incubation reached approximately 6 - 9-fold, while the control cells showed an approximately 12-fold increase. These results indicate that fucoidan inhibited cell growth and viability when the cells were treated with fucoidan upon seeding.

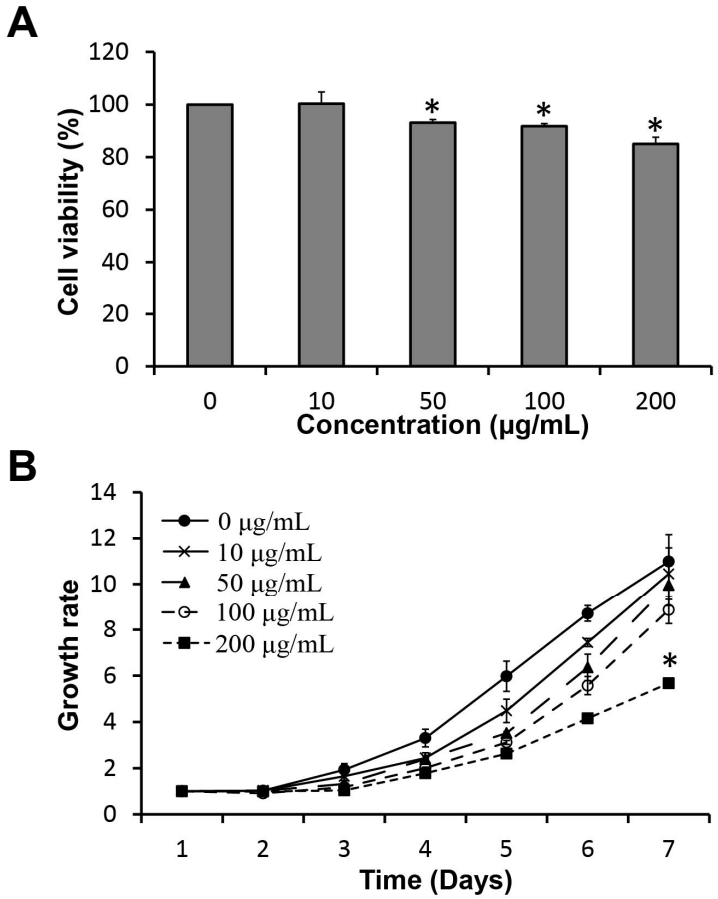

Figure 6. Effect of fucoidan on migration of stably attached osteoblasts

(A) Cell viability in the presence of fucoidan. The harvested MG-63 cells were treated with various concentrations of fucoidan in serum-free medium containing 2% FBS for 12 h and then cell viabilities were measured by MTT assay. The data are the means ± SEM of three experiments (*p<0.05 compared to the control) (B) Growth rates of the cells in the presence of fucoidan. MG-63 cells were plated and incubated in 24-well plates containing different concentrations of fucoidan for 7 days. The number of the cells in the well was counted every 24 h. The data shown are the means ± SEM of three experiments (*p<0.05 compared to the control.)

III-4. Osteosarcoma MG-63 cells are aggregated and rounded by fucoidan treatment

While culturing the cells in presence of fucoidan to measure the growth rate, morphological changes in the cells, such as aggregation and rounding, were observed. It was previously reported that fucoidan treatment results in rearrangement of the cytoskeleton and morphological changes in osteoblastic MC3T3-E1 cells. Thus, I examined the morphological changes of osteosarcoma MG-63 cells in the presence of fucoidan by measuring the area and circularity of the cells (Fig. 7). The cells were treated with various concentrations of fucoidan upon seeding and then incubated for 12 h. The control cells, which were cultured in media without fucoidan, showed highly spread morphology with sharp protrusions around the cells over an area of approximately 500 μm^2. In contrast, in the presence of fucoidan, the cells shrank and became rounded. Most of the cells aggregated and rounded in 100 - 200 μg/mL of fucoidan, while a small number of cells aggregated in 10 - 50 μg/mL of fucoidan. The area of the cells decreased to approximately 150 μm^2 following treatment with 100 - 200 μg/mL of fucoidan, in contrast to that of control cells (500 μm^2). The circularity of the cells was increased by fucoidan treatment in a dose dependent manner. The circularity of the control cells was approximately 0.4, whereas fucoidan-treated cells exhibited highly increased circularity of 0.6 - 0.8 (Fig. 7D). These morphological changes following fucoidan treatment were more clearly observed in the scanning electron microscopy images of the cells after 12-h incubation in 100 μg/mL of fucoidan (Fig. 7E). All cells in the media without fucoidan were spread on the plates, while fucoidan-treated cells were rounded and formed large aggregates.

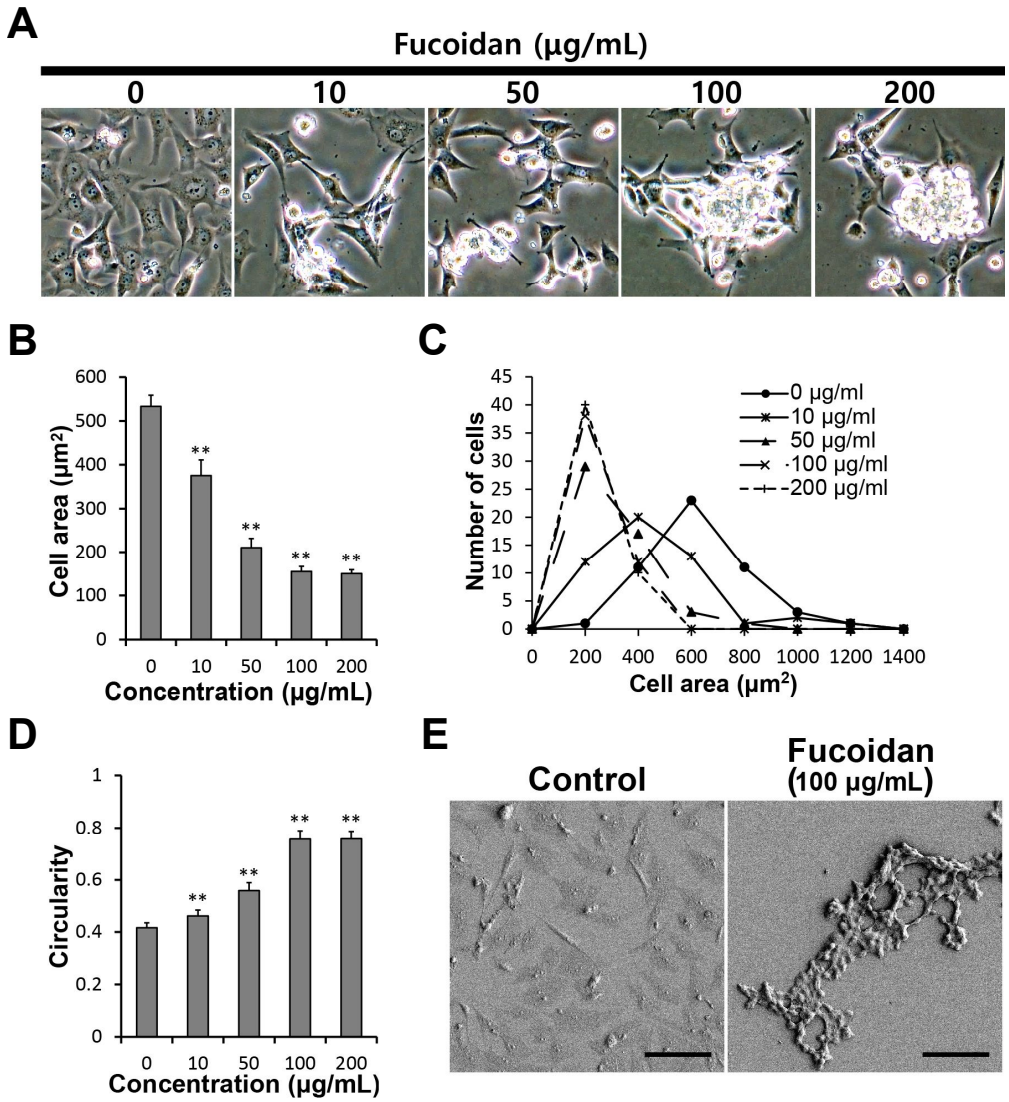

Figure 7. Aggregation morphology of MG-63 cells by frucoidan treatment.

(A) Morphological changes of MG-63 cells in the presence of fucoidan. MG-63 cells were cultured in the presence of various concentrations of fucoidan for 12 h. (B) Quantification of cell area. The sizes of the cells were measured by ImageJ software. (C) Histogram of cell area in different concentrations of fucoidan. (D) Quantification of circularity. Circularity was calculated by 4π *area/perimeter^2. A value of 1.0 indicates a perfect circle. As the value approaches 0.0, it indicates an increasingly elongated shape. The data were presented as the mean ± SD. (E) Images of scanning electron microscopy. Cells on cover glasses treated with 100 μg/mL of fucoidan for 12 h were imaged. Scale bar, 100 μm.

To examine the detailed morphological changes of the cells following fucoidan treatment, I cultured MG-63 cells in the presence of 100 μg/mL of fucoidan for 24 h (Fig. 8). Immediately after seeding, all cells were rounded and small regardless of whether fucoidan was in the media. During incubation, most of the control cells attached to the plate and became spread forming protrusions within 8 h of incubation. In contrast, in the presence of 100 μg/mL of fucoidan, some cells were attached and spread similar to the control cells, but most cells remained unattached and were rounded. The area of fucoidan-treated cells was slightly increased at 4 - 8 h incubation, but subsequently decreased to close to the initial levels (Fig. 8B). While the control cells showed a gradual decrease in the circularity during incubation, fucoidan-treated cells exhibited a slight decrease initially, but became rounded again to the original level (Fig. 8C). These results demonstrate that fucoidan treatment resulted in morphological changes in osteosarcoma cells which were shrunken and rounded.

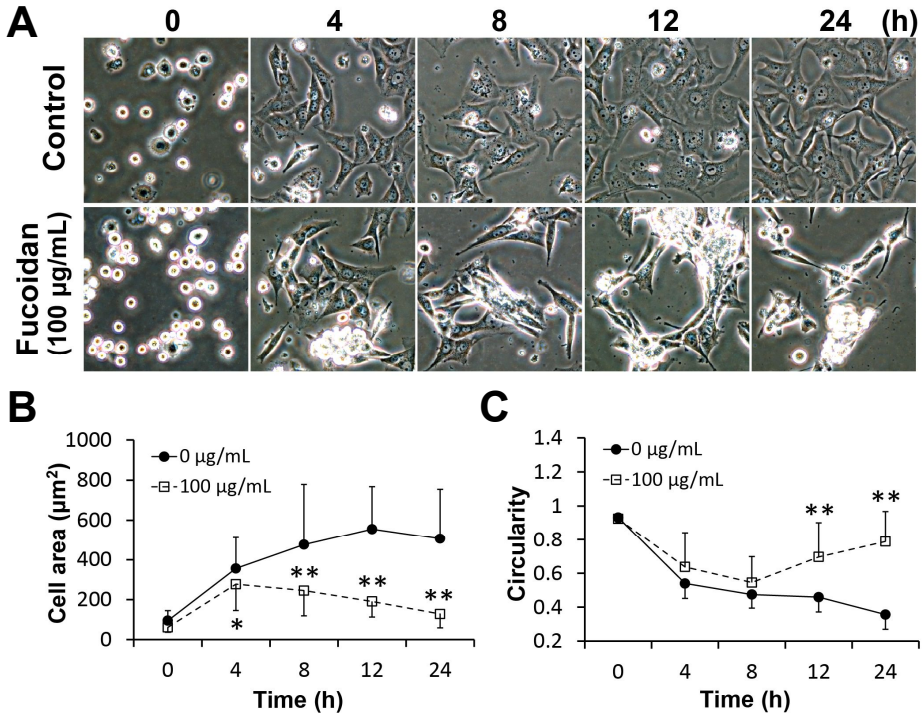

Figure 8. Morphological changes of MG-63 cells following fucoidan treatment.

(A) Morphology of MG-63 cells in the presence of fucoidan (100 μg/mL). MG-63 cells were treated with 100 μg/mL of fucoidan upon seeding before stably attached to the plate and the images were taken every 4 h. The control cells were grown in the absence of fucoidan. (B) Quantification of cell area. (C) Quantification of circularity. The data were presented as the mean ± SD.

III-5. Fucoidan Induces rearrangement of the cytoskeleton in MG-63 cells

Next, I investigated the effects of fucoidan on the cytoskeleton. Harvested cells were treated with fucoidan for 12 h and then fixed and stained with phalloidin to detect the F-actin distribution in the cells (Fig. 9). The control cells, which were not treated with fucoidan, showed highly spreading morphology and numerous protrusions. F-actin in these control cells was relatively evenly distributed around the cells, and showed low accumulation in the center of the cells. Some stretched stress fibers were also detected in control cells. In contrast, fucoidan-treated cells showed high accumulation of F-actin at the rounded cortex and lost stress fibers and protrusions around the cells. The quantification of F-actin in the cytoskeletal fraction revealed a significant increase in F-actin in fucoidan-treated cells compared to in control cells. These results suggest that fucoidan treatment results in the accumulation of F-actin at the cell cortex, leading to rounding of the cells.

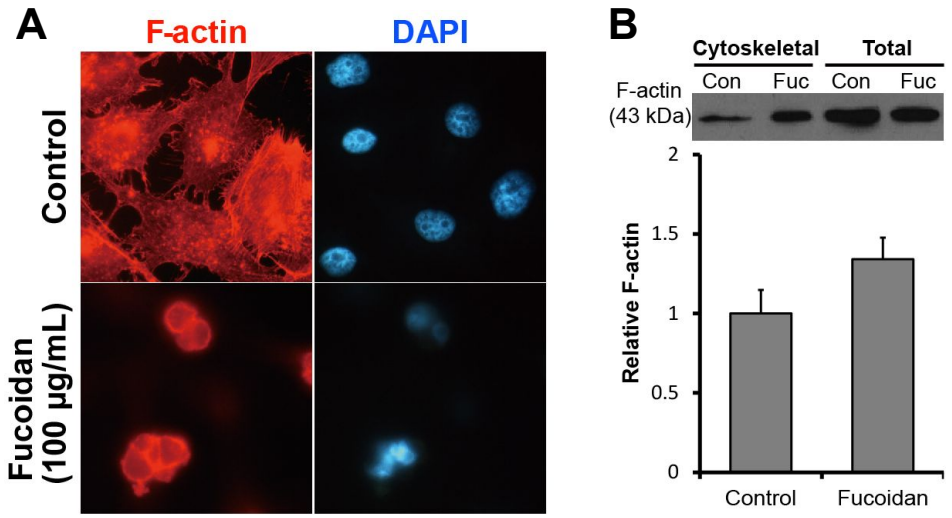

Figure 9. Rearrangements of F-actin in fucoidan-treated cells.

(A) F-actin and nuclei staining. F-actin and nuclei in MG-63 cells were stained with TRITC-phalloidin and Hoechst dye, respectively. MG-63 cells were treated with 100 μg/mL of fucoidan for 12 h. (B) Quantification of F-actin. Total proteins and cytoskeletal fractions from fucoidan-treated cells were extracted and immunoblotted with anti- β -actin antibodies. Densities of the bands were quantified and were expressed as relative amount of F-actin in the cytoskeletal fractions to that in total proteins.

III-6. Fucoidan induces apoptosis in osteosarcoma MG-63 cells

In the previous experiments, the cell viability and growth rate of osteosarcoma cells were inhibited by fucoidan treatment. Apoptotic cells typically show rearrangement of the cytoskeleton. These results suggest that fucoidan has an apoptotic effect. Thus, I examined the apoptotic effects of fucoidan on MG-63 cells using Hoechst 33258 staining and annexin V/propidium iodide (PI) staining (Fig. 10). When the cells were stained with Hoechst 33258, typical morphological characteristics of apoptotic cells, such as chromatin condensation and nuclear fragmentation, were observed in fucoidan-treated cells, while an intact nuclear structure was observed in control cells. These findings were confirmed in an annexin V/PI apoptosis assay. The percentage of annexin V-positive cells, which were apoptotic cells, was significantly increased following fucoidan treatment in a dose-dependent manner. The percentage of apoptotic cells was increased to 20 - 30% when the cells were exposed to 100 or 200 μg/mL of fucoidan for 12 h. However, there was no change in the number of PI-stained cells following fucoidan treatment. These data indicate that fucoidan induces apoptosis in osteosarcoma MG-63 cells.

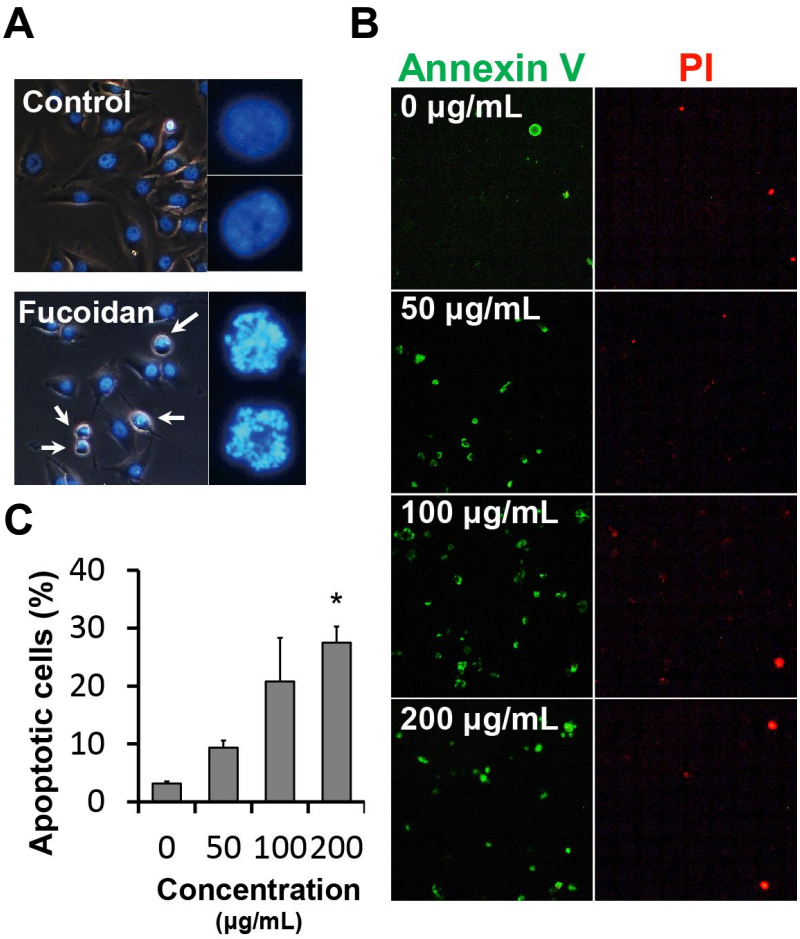

Figure 10. Apoptotic features of fucoidan-treated MG-63 cells.

(A) Chromatin condensation of fucoidan-treated cells. Nuclei of MG-63 cells, which were treated with 100 μg/mL of fucoidan for 12 h, were stained with Hoechst 33258. Arrows indicate nuclei showing condensed chromatin. Enlarged images were shown on the right. (B) Annexin V/ PI staining. MG-63 cells were left untreated or treated for 12 h with different concentrations of fucoidan. Annexin V was visualized by a green, and PI was visualized by a red. (C) Quantification of annexin V-positive cells. The numbers of annexin V-positive cells and total cells were counted, and the apoptotic cells were expressed as percentages of annexin V-positive cells to total cells.

IV. Discussion

The recruitment of osteoprogenitor cells to the sites of bone formation is essential for bone development and rearrangement (Dirckx et al., 2013). Fucoidan is a polysaccharide containing fucose and sulfate groups. Even though fucoidan has been reported to induce osteoblastic differentiation of preosteoblastic cells and is considered a candidate biomaterial for additions to bone tissue-engineered scaffolds (Changotade et al., 2008; Cho et al., 2009; Jeong et al., 2013), little is known about the effects of fucoidan on cell migration. Here, I first examined the effects of fucoidan on the migration of preosteoblastic cells using a wound healing assay. The level of inhibition of migration seems to be proportional to the concentration of fucoidan. These results suggest that fucoidan inhibits migration of the cells when the stably attached cells are treated with fucoidan. In the transwell migration assay, even though the fully grown cells on the plates were starved for 12 h as in the wound-healing assay, there was a difference in the time at which the cells were treated with fucoidan. In the transwell assay, starved cells that were stably attached to the plates were harvested and then placed in the upper container containing fucoidan, while in the wound healing assay the starved cells were not harvested and were treated with fucoidan directly. These results suggest that fucoidan increases migration of the cells when the cells are treated with fucoidan upon seeding after harvesting, but not after they are stably attached to plates. The fucoidan-treated cells in this condition aggregated and appeared to adhere to the plates very weekly. This result suggests that fucoidan may promote the migration of preosteoblastic cells, but that its effects on migration depend on whether cells are treated before or after they stably attached to plates. In agreement with our results, it has been reported that chemotaxis of canine peripheral blood polymorphonuclear cells was increased by fucoidan treatment (Kim et al., 2013). However, there are several studies showing that

fucoidan suppressed migration of diverse types of cancer cells. Fucoidan is suggested to have an anti-tumor effect to inhibit the growth and invasion of several cell lines (Boo et al., 2013; Cho et al., 2014; Lee et al., 2012; Park et al., 2013; Senthilkumar et al., 2013). These present results provide an important suggestion that fucoidan may promote the migration of osteoblasts and that its effects on cell migration vary depending upon the conditions under which cells are treated. The harvested cells may have shown increased migration relative to stably attached cells due to differences in the sensitivities of these cells to extracellular fucoidan. The decrease of adhesion and spreading of the cells is likely to be correlated to the rounded and shrunk morphology of the cells in the presence of fucoidan. Quantification of the amount of F-actin in the cytoskeleton fraction showed a slight increase of F-actin in fucoidan-treated cells. Cytoskeleton rearrangement is mediated by many signaling molecules including chemoattractants, the Rac and Rho signaling pathways, PI3K, and the Akt pathway (Insall, 2013; Lee and Jeon, 2012; Ridley et al., 2003). These dates suggest that fucoidan treatment results in an accumulation of F-actin at the cell cortex in osteoblasts and affects rearrangement of F-actin cytoskeleton. Fucoidan has already been reported to induce activation of Akt signaling (Cho et al., 2014) and somehow to be involved in the PI3K signaling pathway (Boo et al., 2013; Lee et al., 2012). Further studies that determine which signaling molecules, such as PI3K and Akt, are involved in accumulation of F-actin at the cell cortex in fucoidan-treated osteoblasts would be helpful for understanding the cellular and molecular mechanisms mediating regulation of the cytoskeleton by fucoidan.

In conclusion, these results suggest that fucoidan can promote or suppress the migration of osteoblasts and that the effects of fucoidan on migration vary depending on the conditions under which the cells are treated. The osteoblast cells treated with fucoidan before stable attachment to the plates were rounded and aggregated. These cells showed decreased levels of adhesion and an accumulation of F-actin at the rounded cell

cortex. The rearrangement of F-actin in the presence of fucoidan appears to be correlated to changes in cell morphology, adhesion, and migration, which remain to be studied. The First study may provide insights into the effects of fucoidan on bone repair and regeneration.

The study of osteosarcoma MG-63 cells demonstrates that fucoidan induces apoptosis in the cells. Fucoidan-treated cells displayed chromatin condensation and nuclear fragmentation, which are typical characteristics of apoptotic cells, and the number of annexin V-positive cells was increased by fucoidan treatment in a dose-dependent manner. In accordance with these results, the cell viability and growth rate were significantly decreased in the presence of fucoidan, possibly through morphological changes and apoptosis of the cells. When the cells were treated with fucoidan, F-actin accumulated at the cortex of the cells and spreading was blocked, leading to a rounded morphology without protrusions around the cells.

Fucoidan is a fucose-rich polysaccharide present in the extracellular matrix of brown algae and is reported to possess anticancer activities in many different types of cancer cells, including leukemia, breast cancer, prostate cancer, lung adenocarcinoma, and hepatocellular carcinoma cells (Boo et al., 2013; Park et al., 2013; Senthilkumar et al., 2013; Yang et al., 2013; Zhang et al., 2013). Hepatocellular carcinoma cells exposed to fucoidan displayed growth inhibition and apoptosis via the reactive oxygen species-mediated mitochondrial pathway (Yang et al., 2013). Leukemia cells showed fucoidan-induced apoptosis through activation of p38 MAPK and modulation of Bcl-2 family proteins (Park et al., 2013). Prostate cancer and breast cancer cells were reported to undergo apoptosis and growth inhibition following fucoidan treatment (Boo et al., 2013; Zhang et al., 2013). The present study demonstrates that fucoidan has apoptotic effects on human osteosarcoma cells when the cells are treated with fucoidan upon seeding before becoming stably attached to the plates.

Fucoidan was recently reported to have beneficial effects on the cell differentiation and mineralization of osteoblastic cells and radio protective effects on bone marrow cells (Byon et al., 2008; Cho et al., 2009; Park et al., 2012). Fucoidan was reported to stimulate the antigen-presenting functions of dendritic cells and increase the viability of bone marrow cells by inhibiting radiation-induced apoptosis. In first study, I found that the effects of fucoidan on the migration and morphology of osteoblastic cells varied depending on the conditions of cell treatment. When the harvested osteoblastic cells were treated with fucoidan upon seeding, the fucoidan-treated cells exhibited severe morphological changes and became rounded, whereas fucoidan had no clear effects on stably attached osteoblastic cells on the plates including cell viability and morphology. In agreement with these results, the cell viability and growth rate were not affected at low concentrations of fucoidan, and stably attached osteosarcoma cells displayed no clear morphological changes by fucoidan treatment (data not shown).

Conclusion

PART I. Study on Asymmetric Distribution of RapGAP3 During Cell Migration in *Dictyostelium*

I have determined the minimally required amino acids in the I/LWEQ domain of RapGAP3 for posterior localization in migrating cells. More importantly, I found that the minimal region of the protein required for posterior localization (LD10) could localize to the anterior with some additional deletion of its C-terminal (LD11), indicating that the same F-actin binding domain can be modulated to localize to the anterior or posterior of the cell through small protein fragments.

PART II. Study on Fucoidan-Mediated Cell Polarization in Osteoblasts

I have found that the effects of fucoidan on the migration and morphology of osteoblastic cells varied depending on the conditions of cell treatment. In addition, I found that fucoidan appears to have both non-toxic beneficial and cytotoxic apoptotic effects on the cells depending on the conditions of cell treatment.

References

Artemenko, Y., Lampert, T.J., and Devreotes, P.N. (2014). Moving towards a paradigm: common mechanisms of chemotactic signaling in Dictyostelium and mammalian leukocytes. Cellular and Molecular Life Sciences *71*, 3711-3747.

Boo, H.J., Hong, J.Y., Kim, S.C., Kang, J.I., Kim, M.K., Kim, E.J., Hyun, J.W., Koh, Y.S., Yoo, E.S., Kwon, J.M., *et al.* (2013). The anticancer effect of fucoidan in PC-3 prostate cancer cells. Mar Drugs *11*, 2982-2999.

Bos, J.L. (2005). Linking Rap to cell adhesion. Curr Opin Cell Biol *17*, 123-128.

Bos, J.L., and Zwartkruis, F.J. (1999). Signal transduction. Rhapsody in G proteins. Nature *400*, 820-821.

Byon, Y.Y., Kim, M.H., Yoo, E.S., Hwang, K.K., Jee, Y., Shin, T., and Joo, H.G. (2008). Radioprotective effects of fucoidan on bone marrow cells: improvement of the cell survival and immunoreactivity. J Vet Sci *9*, 359-365.

Cai, L., Makhov, A.M., and Bear, J.E. (2007). F-actin binding is essential for coronin 1B function in vivo. J Cell Sci *120*, 1779-1790.

Chan, K.T., Creed, S.J., and Bear, J.E. (2011). Unraveling the enigma: progress towards understanding the coronin family of actin regulators. Trends Cell Biol *21*, 481-488.

Changotade, S.I., Korb, G., Bassil, J., Barroukh, B., Willig, C., Colliec-Jouault, S., Durand, P., Godeau, G., and Senni, K. (2008). Potential effects of a low-molecular-weight fucoidan extracted from brown algae on bone biomaterial osteoconductive properties. J Biomed Mater Res A *87*, 666-675.

Cho, T.M., Kim, W.J., and Moon, S.K. (2014). AKT signaling is involved in fucoidan-induced inhibition of growth and migration of human bladder cancer cells. Food and Chemical Toxicology *64*, 344-352.

Cho, Y.S., Jung, W.K., Kim, J.A., Choi, I.W., and Kim, S.K. (2009). Beneficial effects of fucoidan on osteoblastic MG-63 cell differentiation. Food Chemistry *116*, 990-994.

de Rooij, J., Zwartkruis, F.J., Verheijen, M.H., Cool, R.H., Nijman, S.M., Wittinghofer, A., and Bos, J.L. (1998). Epac is a Rap1 guanine-nucleotide-exchange factor directly activated by cyclic AMP. Nature *396*, 474-477.

Dirckx, N., Van Hul, M., and Maes, C. (2013). Osteoblast recruitment to sites of bone formation in skeletal development, homeostasis, and regeneration. Birth Defects Res C Embryo Today *99*, 170-191.

Durig, J., Bruhn, T., Zurborn, K.H., Gutensohn, K., Bruhn, H.D., and Beress, L. (1997). Anticoagulant fucoidan fractions from Fucus vesiculosus induce platelet activation in vitro. Thromb Res *85*, 479-491.

Etzrodt, M., Ishikawa, H.C., Dalous, J., Muller-Taubenberger, A., Bretschneider,

T., and Gerisch, G. (2006). Time-resolved responses to chemoattractant, characteristic of the front and tail of Dictyostelium cells. FEBS Lett *580*, 6707-6713.

Galkin, V.E., Orlova, A., Schroder, G.F., and Egelman, E.H. (2010). Structural polymorphism in F-actin. Nat Struct Mol Biol *17*, 1318-1323.

Galkin, V.E., VanLoock, M.S., Orlova, A., and Egelman, E.H. (2002). A new internal mode in F-actin helps explain the remarkable evolutionary conservation of actin's sequence and structure. Curr Biol *12*, 570-575.

Insall, R. (2013). The interaction between pseudopods and extracellular signalling during chemotaxis and directed migration. Curr Opin Cell Biol *25*, 526-531.

Jeon, T.J., Lee, D.J., Lee, S., Weeks, G., and Firtel, R.A. (2007a). Regulation of Rap1 activity by RapGAP1 controls cell adhesion at the front of chemotaxing cells. J Cell Biol *179*, 833-843.

Jeon, T.J., Lee, D.J., Merlot, S., Weeks, G., and Firtel, R.A. (2007b). Rap1 controls cell adhesion and cell motility through the regulation of myosin II. J Cell Biol *176*, 1021-1033.

Jeon, T.J., Lee, S., Weeks, G., and Firtel, R.A. (2009). Regulation of Dictyostelium morphogenesis by RapGAP3. Dev Biol *328*, 210-220.

Jeong, H.S., Venkatesan, J., and Kim, S.K. (2013). Hydroxyapatite-fucoidan nanocomposites for bone tissue engineering. Int J Biol Macromol *57*, 138-141.

Kim, S.H., Kang, J.H., and Yang, M.P. (2013). Fucoidan directly regulates the chemotaxis of canine peripheral blood polymorphonuclear cells by activating F-actin polymerization. Vet Immunol Immunopathol *151*, 124-131.

Kooistra, M.R., Dube, N., and Bos, J.L. (2007). Rap1: a key regulator in cell-cell junction formation. J Cell Sci *120*, 17-22.

Kortholt, A., and van Haastert, P.J. (2008). Highlighting the role of Ras and Rap during Dictyostelium chemotaxis. Cell Signal *20*, 1415-1422.

Kucik, D.F., and Wu, C. (2005). Cell-adhesion assays. Methods Mol Biol *294*, 43-54.

Lee, H., Kim, J.S., and Kim, E. (2012). Fucoidan from seaweed Fucus vesiculosus inhibits migration and invasion of human lung cancer cell via PI3K-Akt-mTOR pathways. PLoS One *7*, e50624.

Lee, M.R., and Jeon, T.J. (2012). Cell migration: regulation of cytoskeleton by Rap1 in Dictyostelium discoideum. J Microbiol *50*, 555-561.

Lee, M.R., Kim, H., and Jeon, T.J. (2014). The I/LWEQ domain in RapGAP3 required for posterior localization in migrating cells. Mol Cells *37*, 307-313.

Maiuri, P., Rupprecht, J.F., Wieser, S., Ruprecht, V., Benichou, O., Carpi, N., Coppey, M., De Beco, S., Gov, N., Heisenberg, C.P., *et al.* (2015). Actin flows mediate a universal coupling between cell speed and cell persistence. Cell *161*, 374-386.

McCann, R.O., and Craig, S.W. (1997). The I/LWEQ module: a conserved

sequence that signifies F-actin binding in functionally diverse proteins from yeast to mammals. Proc Natl Acad Sci U S A *94*, 5679-5684.

Meng, R., and Xie, L. (2014). Gap junction mediated regulation of osteocytes to osteoblastic alkaline phosphatase activity is independent of microgravity. Animal Cells and Systems *18*, 1-8.

Mun, H., Lee, M.R., and Jeon, T.J. (2014). RapGAP9 regulation of the morphogenesis and development in Dictyostelium. Biochem Biophys Res Commun *446*, 428-433.

Nakahama, K. (2010). Cellular communications in bone homeostasis and repair. Cell Mol Life Sci *67*, 4001-4009.

Nakamura, T., Suzuki, H., Wada, Y., Kodama, T., and Doi, T. (2006). Fucoidan induces nitric oxide production via p38 mitogen-activated protein kinase and NF-kappaB-dependent signaling pathways through macrophage scavenger receptors. Biochem Biophys Res Commun *343*, 286-294.

Nellen, W., Silan, C., and Firtel, R.A. (1984). DNA-mediated transformation in Dictyostelium discoideum: regulated expression of an actin gene fusion. Mol Cell Biol *4*, 2890-2898.

Park, H.S., Hwang, H.J., Kim, G.Y., Cha, H.J., Kim, W.J., Kim, N.D., Yoo, Y.H., and Choi, Y.H. (2013). Induction of apoptosis by fucoidan in human leukemia U937 cells through activation of p38 MAPK and modulation of Bcl-2 family. Mar Drugs *11*, 2347-2364.

Park, S.J., Lee, K.W., Lim, D.S., and Lee, S. (2012). The sulfated polysaccharide fucoidan stimulates osteogenic differentiation of human adipose-derived stem cells. Stem Cells Dev *21*, 2204-2211.

Pignolo, R.J., and Kassem, M. (2011). Circulating osteogenic cells: implications for injury, repair, and regeneration. J Bone Miner Res *26*, 1685-1693.

Retta, S.F., Balzac, F., and Avolio, M. (2006). Rap1: a turnabout for the crosstalk between cadherins and integrins. Eur J Cell Biol *85*, 283-293.

Ridley, A.J., Schwartz, M.A., Burridge, K., Firtel, R.A., Ginsberg, M.H., Borisy, G., Parsons, J.T., and Horwitz, A.R. (2003). Cell migration: integrating signals from front to back. Science *302*, 1704-1709.

Salwinski, L., Miller, C.S., Smith, A.J., Pettit, F.K., Bowie, J.U., and Eisenberg, D. (2004). The Database of Interacting Proteins: 2004 update. Nucleic Acids Res *32*, D449-451.

Sasaki, A.T., Chun, C., Takeda, K., and Firtel, R.A. (2004). Localized Ras signaling at the leading edge regulates PI3K, cell polarity, and directional cell movement. J Cell Biol *167*, 505-518.

Senetar, M.A., Foster, S.J., and McCann, R.O. (2004). Intrasteric inhibition mediates the interaction of the I/LWEQ module proteins Talin1, Talin2, Hip1, and Hip12 with actin. Biochemistry *43*, 15418-15428.

Senthilkumar, K., and Kim, S.K. (2014). Anticancer effects of fucoidan. Adv Food Nutr Res *72*, 195-213.

Senthilkumar, K., Manivasagan, P., Venkatesan, J., and Kim, S.K. (2013).

Brown seaweed fucoidan: biological activity and apoptosis, growth signaling mechanism in cancer. Int J Biol Macromol *60*, 366-374.

Shimozawa, T., and Ishiwata, S. (2009). Mechanical distortion of single actin filaments induced by external force: detection by fluorescence imaging. Biophys J *96*, 1036-1044.

Song, E.K., and Park, T.J. (2014). Integrin signaling in cartilage development. Animal Cells and Systems *18*, 365-371.

Uyeda, T.Q., Iwadate, Y., Umeki, N., Nagasaki, A., and Yumura, S. (2011). Stretching actin filaments within cells enhances their affinity for the myosin II motor domain. PLoS One *6*, e26200.

Wang, J., Zhang, Q., Zhang, Z., Song, H., and Li, P. (2010). Potential antioxidant and anticoagulant capacity of low molecular weight fucoidan fractions extracted from Laminaria japonica. Int J Biol Macromol *46*, 6-12.

Washington, R.W., and Knecht, D.A. (2008). Actin binding domains direct actin-binding proteins to different cytoskeletal locations. BMC Cell Biol *9*, 10.

Weber, I., Niewohner, J., Du, A., Rohrig, U., and Gerisch, G. (2002). A talin fragment as an actin trap visualizing actin flow in chemotaxis, endocytosis, and cytokinesis. Cell Motil Cytoskeleton *53*, 136-149.

Xue, M., Ge, Y., Zhang, J., Liu, Y., Wang, Q., Hou, L., and Zheng, Z. (2013). Fucoidan inhibited 4T1 mouse breast cancer cell growth in vivo and in vitro via downregulation of Wnt/beta-catenin signaling. Nutr Cancer *65*, 460-468.

Yang, L., Wang, P., Wang, H., Li, Q., Teng, H., Liu, Z., Yang, W., Hou, L., and Zou, X. (2013). Fucoidan derived from Undaria pinnatifida induces apoptosis in human hepatocellular carcinoma SMMC-7721 cells via the ROS-mediated mitochondrial pathway. Mar Drugs *11*, 1961-1976.

Zapopozhets, T.S., Besednova, N.N., and Loenko Iu, N. (1995). [Antibacterial and immunomodulating activity of fucoidan]. Antibiot Khimioter *40*, 9-13.

Zhang, Z., Teruya, K., Eto, H., and Shirahata, S. (2013). Induction of apoptosis by low-molecular-weight fucoidan through calcium- and caspase-dependent mitochondrial pathways in MDA-MB-231 breast cancer cells. Biosci Biotechnol Biochem *77*, 235-242.

Acknowledgements

설레는 마음으로 연구실 생활을 시작한지 어제 같은데, 벌써 4년이라는 시간이 흘렀습니다. 처음 연구실에 들어왔을 땐 아무 실험도 할 줄 모르고 팁만 꽂는 것이 마냥 지루했지만, 피펫을 손에 쥐었을 때 그 벅참과 감동이 학위과정에 발을 들여 놓은 계기가 된 것 같습니다. 제가 이렇게 한자리에서 꾸준하게 기술과 지식을 습득할 수 있도록 기회를 주신 저의 지도교수님이신 전택중 교수님과의 인연은 제 인생의 가장 큰 전환점이라고 생각합니다. 학부 과정 전공 수업 중 질문을 만들게 해서 전공지식에 대한 궁금증을 유발하게 해주신 이준식 교수님, 감사합니다. 항상 진지하신 것 같지만 때로는 학생들을 칭찬과 염려해주시는 조광원 교수님, 감사합니다. 세심한 논문 심사로 좋은 학위논문을 만들게 조언해주신 이성행 교수님, 감사합니다. 대학원 학과장이신 정현숙 교수님, 도장받으러 갈때마다 기분좋게 웃어주셔서 고맙습니다. 이정섭 교수님, 저희 교수님 연구년제 가셨을 때, 저희 챙겨주셔서 감사합니다. 자주 뵐 기회는 없었지만, 항상 세미나에서 학생들을 향해 격언과 조언해주시는 조태오 교수님, 송상기 교수님, 박현용 교수님 감사합니다. 가끔 저녁 밥 챙겨주시는 정민주 교수님 감사합니다. 미은 박사님, 박사님 보고 여성과학자의 꿈을 키우고 있어요. 신구오빠, 학교에서 오빠 한 5년 본 것 같은데 말이에요. 졸업하시고 이제 학교에서 안보이면 허전할 것 같아요. 미래언니, 언니 덕분에 처음 들어올 때 어려울 것만 같았던 실험실 생활을 쉽게 다가설 수 있게 친근하게 대해줘서 고마워요. 실험실 동기이자 분위기 메이커인 동엽 오빠, 오빠 덕분에 실험실 분위기가 좋았어요. 내 석사학위 동기 민지야 네가 해준 많은 좋은 말들

잊지 않을게. 어딜 가도 기죽지 말고 힘내 내 친구 파이팅. 놀러 가면 가끔 원두커피 내려주는 호태 오빠, 다음에 병철오빠랑 막창 또 먹으러 가요. 푸름아, 지난번에 해준 떡볶이랑 떡고물 엄청 맛있었어. 비법 좀 메일로 보내주겠니…? 실험실 후배인 병규, 예진이, 지성이 다들 고마워. 덕분에 논문 쓰는데 집중할 수 있었어. 내 학부 동기 은지야 아량아 너흰 졸업하고 먼저 취업하겠구나. 얘들아, 취업 준비 응원할 테니 첫 월급타면 밥 사. 지민이, 현영이, 수민이는 학교에서 더 보자. 인화, 은선이, 다휘 너희도 하는 일 잘 되길 바랄게. 그리고 3년동안 항상 내 옆에 있어준 친구 같고, 아빠 같고, 오빠 같고 아들 같은 내 남자친구 병철 오빠, 2년 반을 매일 같이 정류장까지 바래다주느라 애썼어. 오빠 덕에 항상 퇴근길 안심귀가 했었어. 미운 4살마냥 내가 심술 부리는데도, 도시락 챙겨주고 이벤트 챙겨주고 기념일 챙겨주느라 욕봤어…. 앞으로도 쭉 내 옆에 있어야 해.

마지막으로, 4년동안 학위 과정 하면서 있는 짜증 없는 짜증 다 부렸는데, 다 받아주시고 싫은 내색 한번 안 하시고 내가 하고 싶은 실험에 전념할 수 있도록 뒷바라지 다해주신 아빠, 엄마 감사해요. 어느 길을 선택하든 내 선택에 힘 실어주고, 주변에 나를 추켜세워주며 자존감 높은 사람으로 만들어줘서 항상 고마워요.

긴 글 읽어주셔서 감사합니다. 더 발전하여 제가 누군가의 꿈이 될 때까지 더 많이 노력하겠습니다. 항상 하시는 일 모두 잘되기를 기원하며 석사학위논문을 마칩니다.